Pure appl. geophys. 158 (2001) 1301–1338
0033–4553/01/071301–38 $ 1.50 + 0.20/0

Pure and Applied Geophysics

Calibration of the Regional Crustal Waveguide and the Retrieval of Source Parameters Using Waveform Modeling

CHANDAN K. SAIKIA[1], BRADLEY B. WOODS[1] and H. K. THIO[1]

Abstract — Regional crustal waveguide calibration is essential to the retrieval of source parameters and the location of smaller ($M < 4.8$) seismic events. This path calibration of regional seismic phases is strongly dependent on the accuracy of hypocentral locations of calibration (or master) events. This information can be difficult to obtain, especially for smaller events. Generally, explosion or quarry blast generated travel-time data with known locations and origin times are useful for developing the path calibration parameters, but in many regions such data sets are scanty or do not exist. We present a method which is useful for regional path calibration independent of such data, i.e. with earthquakes, which is applicable for events down to $M_w = 4$ and which has successfully been applied in India, central Asia, western Mediterranean, North Africa, Tibet and the former Soviet Union. These studies suggest that reliably determining depth is essential to establishing accurate epicentral location and origin time for events. We find that the error in source depth does not necessarily trade-off only with the origin time for events with poor azimuthal coverage, but with the horizontal location as well, thus resulting in poor epicentral locations. For example, hypocenters for some events in central Asia were found to move from their fixed-depth locations by about 20 km. Such errors in location and depth will propagate into path calibration parameters, particularly with respect to travel times. The modeling of teleseismic depth phases (*pP*, *sP*) yields accurate depths for earthquakes down to magnitude $M_w = 4.7$. This M_w threshold can be lowered to four if regional seismograms are used in conjunction with a calibrated velocity structure model to determine depth, with the relative amplitude of the P_{nl} waves to the surface waves and the interaction of regional *sPmP* and *pPmP* phases being good indicators of event depths. We also found that for deep events a seismic phase which follows an *S*-wave path to the surface and becomes critical, developing a head wave by *S* to *P* conversion is also indicative of depth. The detailed characteristic of this phase is controlled by the crustal waveguide. The key to calibrating regionalized crustal velocity structure is to determine depths for a set of master events by applying the above methods and then by modeling characteristic features that are recorded on the regional waveforms. The regionalization scheme can also incorporate mixed-path crustal waveguide models for cases in which seismic waves traverse two or more distinctly different crustal structures. We also demonstrate that once depths are established, we need only two-stations travel-time data to obtain reliable epicentral locations using a new adaptive grid-search technique which yields locations similar to those determined using travel-time data from local seismic networks with better azimuthal coverage.

Key words: Location, depth determination, waveform modeling.

[1] URS Group, Inc., 566 El Dorado Street, Pasadena, CA 91101, U.S.A.
E-mail: chandan_saikia@urscorp.com

Introduction

Recent studies have demonstrated that regional path calibration is essential for obtaining accurate locations of seismic events at all magnitudes (RUSSIAN FEDERATION/UNITED STATES CALIBRATION WORKING GROUP, 1998; SAIKIA *et al.*, 1996a, b; THIO *et al.*, 1999; ZHU *et al.*, 1997; RYABOY, 1999). Accurate locations are integral to Comprehensive Test-Ban Treaty (CTBT) seismic monitoring efforts, particularly for smaller events, and are also crucial to many types of calibration studies. RYABOY (1999) has demonstrated that applying corrections for regionalized velocity models to the travel times of regional phases from nuclear explosions reduces location errors significantly, putting the relocations on par with announced event locations. Smaller ($M < 5$) events may only be recorded by a few stations, often with poor azimuthal coverage; consequently their hypocenter error ellipses can be extremely large, especially when located by only a few teleseismic observations (BONDÁR, 1998). At even lower magnitude levels the issue of signal-to-noise ratio (SNR) poses a problem for picking first arrivals. SAIKIA *et al.* (1996a) have demonstrated that the arrival times of teleseismic *P* waves may have timing errors up to several seconds for small events ($m_b \approx 4$), even after the stacking of array data, although such events are well recorded at closer regional distances ($\Delta \leq 10°$). Therefore regionalized velocity models for locating events with closer-in observations become necessary.

In addition, a crustal velocity model which can generate the recorded characteristics of regional phases is also useful for inverting regional waveforms in order to retrieve source parameters of earthquakes (e.g., LANGSTON and HELMBERGER, 1975; SAIKIA and HERRMANN, 1985; ZHAO and HELMBERGER, 1994; DREGER and HELMBERGER, 1993; SAIKIA and HELMBERGER, 1993; ZHU and HELMBERGER, 1996; RODGER and SCHWARTZ, 1998), particularly for smaller events ($M < 5$), which are difficult to analyze teleseismically because of the SNR thresholds. Such source information can directly be used for event identification. For example, seismic moment (M_0) which is a resultant product of the source inversion, is an essential parameter in some discriminants such as m_b:M_0 (PATTON and WALTER, 1993) and M_L:M_0 (WOODS *et al.*, 1993). M_0 is also an important parameter for accurate single-station path calibrations of regional seismic-phase amplitudes used for discrimination (PRIESTLEY and PATTON, 1997) and reliable magnitude measurements.

Furthermore, regional analysis of shallow crustal events can improve source depth estimates as teleseismic *P* waves can be contaminated by source-end upper-crustal reverberations, making it difficult to identify emergent first arrivals (STEIN and WIENS, 1986; THIO *et al.*, 1999). Well calibrated regional crustal waveguides are also important to modeling or inversion of teleseismic *P* waves (*P*, *pP* and *sp*) to determine source depth (NELSON *et al.*, 1987; WOODS *et al.*, 1998), as teleseismic *P*-wave based hypocenters can have significant error in depth, even for larger events ($M_w > 5$). Thus modeling the regional crustal waveguide is not only critical to accurate source analysis of smaller events ($4 \leq M_w \leq 5$), but is also useful for locating

events of all sizes, particularly with respect to depth. Both hypocentral location and source parameter information are important ground-truth information for various calibration efforts, as well as for understanding earthquake source phenomenology.

In general, the crustal waveguide of a region can readily be calibrated, with respect to travel time and amplitude of predominant regional seismic phases, provided there exists a set of master events for which ground-truth (GT) locations and origin times are available (BONDÁR, 1998). The best events for travel-time calibration are announced nuclear explosions or quarry blasts for which reliable shot times and locations are available. Unfortunately for most regions, explosions or quarry blasts only cover a few source-specific station paths and often are not available at all for many areas. In lieu of such events, well located earthquakes are required. Earthquakes whose hypocenters are determined using the *P* and *S* arrivals from the local network stations with adequate azimuthal coverage are ideal because they are based on the velocity models that are consistent with travel times of local and regional seismic phases. However, not all regions have such comprehensive networks and so other means must be used to obtain the near GT source information. In such cases the modeling of broadband regional waveforms can be very useful in constraining hypocentral locations as well as other source information. Finding accurate depths is essential for ground-truth events because errors in depths can also result in inaccurate estimates of calibration parameters such as the station-specific-source corrections (SSSC).

Regional records, however, are generally more complicated than teleseismic signals due to the greater influence of upper-crustal heterogeneities (DREGER and HELMBERGER, 1993; SAIKIA, 1994) which gives rise to additional reflected and converted body-wave phases, particularly at shorter periods and thus can require considerable modeling. Additionally, lateral variations in the crustal structure give rise to significant travel-time residuals relative to a single uniform crustal waveguide model for a large area such as North America (ROMNEY *et al.*, 1962). Regional surface waves are also sensitive to lateral variations in the crustal waveguide, particularly Moho depth and the thickness of low velocity sedimentary layers in the upper crust, indicating the importance of possible sub-regionalization of such models (SAIKIA and HELMBERGER, 1993; THIO and KANAMORI, 1995; WOODS *et al.*, 1998) for areas in which one crustal model will not suffice.

In this paper we will review methods that use regional seismograms for calibrating regional waveguides in areas where there is a lack of earthquakes with reliable hypocentral locations. These methods were successfully used in calibrating crustal structure and locating earthquakes in the Pamir Hindu-Kush region (ZHAO and HELMBERGER, 1992; SAIKIA *et al.*, 1996a, b; ZHU *et al.*, 1997), western Mediterranean and North Africa (THIO *et al.*, 1999), the former Soviet Union (SAIKIA and HELMBERGER, 1993), southern California (DREGER and HELMBERGER, 1993; ZHU and HELMBERGER, 1996) and central Asia (WOODS *et al.*, 1998). This modeling of potentially complicated regional waveforms to obtain a crustal waveguide structure is

facilitated by independent estimates of earthquake source depth, orientation and seismic moment so that these effects can be correctly included in the synthetic seismograms. The accuracy and applicability of this information from various techniques and sources shall also be discussed. We will describe a procedure for modeling crustal structure using regional waveforms in conjunction with source constraints from other seismic methods, and provide examples of results from our more recent studies as well as comparisons with results from other sources.

Methodology

In order to model the crustal waveguide with regional seismograms, it is important to have accurate focal mechanisms and source depths for the master events so that these effects can be correctly accounted for generating synthetic seismograms to match the observed waveforms. The calibration, or master, earthquakes used for this purpose are preferably larger events in the $5 \leq M_w \leq 6$ range. Events of this size should be well recorded teleseismically, thereby providing locations which can meet the GT5, GT10 or GT25 criteria (BONDÁR, 1998). Such large events will also provide necessary seismograms for determining focal depth and source parameters at all ranges. Earthquakes much larger than $M_w = 6$, though well recorded, tend to have more complex source processes for which the seismograms can be complex to model unless the source process is successfully deciphered, whereas events smaller than this have relatively simple source processes which can be approximated with a simple source-time function; hence are useful as master events. The events that have been modeled to data are small in magnitude ($M_w \leq 5.5$) and we have used just triangular source functions in modeling their waveforms.

In general, earthquakes ($M_w \geq 5$) which satisfy the criteria for master events have their source parameters, namely the seismic moment and focal mechanisms, readily available. Surface-wave centroid-moment-tensor (CMT) solutions are often available for $M_w \geq 5.5$ events globally from the Harvard catalog (DZIEWONKSI *et al.*, 1981). Recently ARVIDSSON and EKSTRÖM (1998) have extended the global CMT analysis to moderate-sized ($M_w \geq 4.5$) earthquakes using shorter period (40–150 sec) waveforms. Regional results are also being routinely compiled by a number of groups (RITMESA and LAY, 1993; THIO and KANAMORI, 1995; GEE *et al.*, 1996) and as more broadband seismic networks become operational, the number of regional CMT catalogs should also grow. In addition, literature reviews of regional source studies which make use of regional surface waves as well as regionalized earth models should also provide a wealth of information for potential master events. Teleseismic body-wave CMT inversions (SIPKIN, 1982) also provide well constrained solutions, particularly if they include analysis of *S* waves; although such catalogs are less extensive. However, there are numerous regional source studies in the literature which use similar teleseismic analysis. Furthermore, teleseismic studies which model,

or invert, the phases *P*, *pP*, and *sP* (ZHAO and HELMBERGER, 1991a; STEIN and WIENS, 1986) provide the best estimates of focal depth; other methods are more susceptible to error. This subject is discussed in more detail below.

Teleseismic location and depth estimates are known to contain appreciable errors. ISC locations are determined primarily from first arrival *P* waves (ADAMS *et al.*, 1982). Secondary phases, in particular *pP* and *sP*, are used to constrain depth only when the *P*-wave inversion does not converge. This depth phase analysis, however, is not done with regionalized models, but with a single generic global velocity model. Therefore, the depth is sometimes not well determined and is often assigned a fixed value for many events. RÖHM *et al.* (1999) found significant delays in ISC travel-time data which they attribute to errors in the picking of arrival times or the timing of data. BILLINGS *et al.* (1994) conclude that the sensitivity of *P* arrivals to changes in depth are swamped by model errors and, therefore, the inclusion of depth phases such as *pP* is highly recommended. They also found that the effect of picking phase arrival errors on location is considerably smaller than the mislocation caused by lateral variations when only the direct *P* arrivals are used. RÖHM *et al.* (1999) found temporal variations in median station delays on the order of 0.5–1.0 seconds which, because of its systematic nature, may introduce biases in locations, particularly since the biases are often shared by stations in a given regional network.

It is well established that ISC and PDE depth estimates can contain major errors, particularly for small and shallow crustal earthquakes. Recent relocation studies have shown significant differences in location and depths relative to the corresponding ISC values. In a relocation of 60 Tibetan earthquakes using short- and long-period teleseismic waveform modeling, ZHAO and HELMBERGER (1991a) found the majority of events' depths moved to the upper 20 km of the crust, whereas the ISC depths had a more random distribution throughout the top 60 km of the crust. Although the hypocentral locations did not move significantly, the origin times decreased by an average of 3 seconds due to the trade off in the focal depth and station corrections in the travel times. Using regional waveforms, ZHU *et al.* (1997) found crustal earthquakes in the Hindu-Kush region on average to be 17 ± 19 km shallower than their ISC estimates, while mantle earthquakes ($h > 100$ km) only moved by about 8 ± 18 km upwards relative to their ISC depths. Teleseismic *P*-wave depth estimates for shallow earthquakes are generally considered to have larger errors as that is where the largest variations in source structure are, and crustal events tend to generate more scattered phases which can make picking the initial *P* wave and other depth phases more difficult, especially for smaller events and for records with emergent *P*-wave first arrivals (STEIN and WIENS, 1986). In a comprehensive relocation of $M_w \geq 5.2$ events, using available secondary phases, ENGDAHL *et al.* (1998) found that the average depth decreased by less than 2 km relative to ISC values, however, the standard deviation was 12 km, suggesting considerable scatter between the two sets of depth estimates. Further, events for which depth shifts were greater than 40 km (approximately 2% of the data) were not included in the analysis,

thus the overall average depth shift may well be larger. Hypocenters moved by less than 7.5 ± 5.5 km, on average, which is within the estimated ISC location errors.

Surface-wave centroid-moment-tensor (CMT) solutions are also susceptible to errors in depth estimates which, in turn, can give rise to errors in M_0. A significant portion of global CMT solutions for crustal earthquakes have depths fixed at 10, 15 or 33 km (SAIKIA *et al.*, 1997). On average the CMT hypocenters are mislocated by over 30 ± 20 km relative to the relocations of ENGDAHL *et al.* (1998). Globally, the focal depths are on average only 2 ± 13 km shallower than the relocated depths. However, again the variance is large and regional variations can be more significant. For example, in the Tien Shen region of northwest China, regional surface-wave spectra-inversion for 26 earthquakes relocated the events 2 km shallower on average than the CMT depths (PATTON, 1998). In a study of the same events, WOODS *et al.* (1998) found that depths determined from a combination of *P*-wave depth-phase waveform modeling and regional waveform inversion yielded source depths that were respectively 8 and 5 km shallower, on average, than the CMT depths. The ISC focal depths were generally deeper. Another regional waveform source inversion study found similar depth differences for the available CMT comparisons (GHOSE *et al.*, 1998).

Accurate source depth helps to constrain the epicentral location by minimizing the trade-off between source depth and origin time, so that absolute travel-time calibrations are improved. Source depth has a strong influence on the impulsiveness and amplitude of regional body waves, with deeper events having sharper, more impulsive arrivals and fewer scattered phases. The excitation functions of fundamental-mode surface waves are also depth dependent, with deeper events generating relatively smaller amplitude waves. Thus a priori depth information is important for determining regional waveguide Green's functions. Ground-truth depth, of course, is an important parameter in the source discrimination studies (WALTER *et al.*, 1995; TAYLOR, 1995; PRIESTLEY and PATTON, 1997; VÖGFORD, 1997; GUPTA *et al.,* 1997) as many source phenomena have direct or indirect depth dependence such as source medium material properties (WALTER *et al.*, 1995).

M_0 is an important parameter for calibrating amplitude-distance corrections. Absolute amplitude information is required of any single-station calibration method, including empirical distance corrections, measures of attenuation, waveform modeling, and spectral amplitude fitting. As surface-wave excitation functions are source-depth dependent, there exists a trade-off between focal depth and seismic moment. Furthermore, M_0 is also earth-model dependent. Consequently, discrepancies between teleseismic Harvard CMT moments (DZIEWONSKI *et al.*, 1981), which use a generic PREM crust ($h = 24.4$ km) to determine the surface wave source excitation functions, and regional M_0 estimates, based on more appropriate earth models with thicker crusts, are expected to arise. Such biases in CMT moment estimates have been found in several regions. The surface wave-spectra inversion using a regional crustal model also yielded seismic moments 0.27 log units lower than Harvard CMT

solutions (PATTON, 1998). The cause was attributed to the difference in source depth as discussed above and to the difference between the PREM and the regional crustal models for the area, for which the Moho depth ranges between 45 and 60 km. Similarly, regional moments of Hindu-Kush earthquakes were also lower than the CMT values by 0.33 units (ZHU *et al.*, 1997), with the largest differences for the crustal events, as was noted by PATTON (1998). Here the crust is estimated to be 70 km thick.

Focal mechanisms of CMT solutions tend to be well determined, generally agreeing with teleseismic first-arrival and waveform modeling solutions (WOODS *et al.*, 1998) as well as well-constrained regional estimates (ZHU *et al.*, 1997; ZHAO and HELMBERGER, 1991b). In regions of extreme lateral variation in the crust, regional and teleseismic CMT source mechanisms are less compatible as was found to be the case in the western Mediterranean (THIO *et al.*, 1999). But, in general, these long-period teleseismic CMT solutions are adequate for correcting for mechanism effects in the regional waveform modeling. When possible, source mechanism information determined from regional data should be complemented with teleseismic body-wave waveform inversion solutions. For large events ($M_w \geq 5.5$) and, in some cases, slightly lower magnitude ones (down to $M \geq 5$), teleseismic source determinations combining *P*- and *S*-wave waveforms can provide well constrained solutions whereas, for example, first-motion mechanisms can differ by as much as 45° in strike and rake for the same earthquake, depending on the data if local station data are unavailable (NELSON *et al.*, 1987).

In order to obtain the reliable source information for master events to calibrate a regional waveguide, it is important to use teleseismic body wave observations to determine depth and source parameters. The relative time separation of *pP* and *sP* waves from the *P* waves helps to constrain focal depth, while their amplitudes along with *S* waves provide accurate estimates of focal mechanism and M_0. Although the character of these teleseismic waveforms is dependent on the source and receiver crustal structures, it is less sensitive to the details of regional waveguide than that of surface waves and regional body waves. Using the standard technique of generalized ray theory (LANGSTON and HELMBERGER, 1975), synthetic teleseismic seismograms can be generated in the range of 30° to 90° for which the ground motion displacement is approximated by

$$W_{Z,R}(t) = R_{(pZ,pR)}\left[\frac{\mathrm{d}\phi}{\mathrm{d}t} + R_{pP}\frac{\mathrm{d}\phi}{\mathrm{d}t}\cdot H(t-\Delta t_1) + R_{sP}\frac{\mathrm{d}\psi}{\mathrm{d}t}\cdot H(t-\Delta t_2)\right]$$

where $\mathrm{R}_{(pZ,pR)}$ represents the vertical or radial receiver function, R_{pP} and R_{sP} are the respective *P*- and *S*-wave free-surface reflection coefficients, Δt_1 and Δt_2 are time lags of *pP* and *sP* relative to the mantle *P* waves, η_α and η_β are vertical slowness for *P* and *S* waves, and $H(t-\Delta t)$ is the time-lagged heavy-side step function; ϕ and ψ are displacement potentials and their detailed expressions can be found in LANGSTON and HELMBERGER (1975), as well as the similar expressions for the *S*-wave ground

motions. The synthesized ground motions are convolved with the source time function and attenuation model. The source radiation affect is also added prior to comparing with the instrument-deconvolved observations.

Another approach to generate teleseismic seismograms is utilization of the Thomson-Haskell propagator matrix method (HASKELL, 1962; AKI and RICHARDS, 1980) to propagate the wavefield through the source and receiver regions. We developed a code to compute synthetic Green's functions for the fundamental faults following this approach in which geometrical spreading of the seismic rays and the anelasticity of the earth are accounted for separately, using the formulation presented in BEN-MENAHEM *et al.* (1965) and TENG and BEN-MENAHEM (1962). We propagate the wavefield using the formulation presented in HUDSON (1969) where the Haskell layer 4×4 matrices have been modified to the of format 6×6 compound matrices (SAIKIA, 1994) and used a complex frequency. Unlike in the generalized ray approach, this method needs no specification of rays as it includes the total wavefield. The code calculates the ray parameters for the teleseismic paths using the J-B travel-time table and requires only the receiver and source locations.

The teleseismic source mechanisms of master events are inverted using the Green's functions generated as described above by performing a grid search sweeping through focal-mechanism parameter space of strike, dip, and slip to obtain the best mechanism at each depth. Depth is constrained by fitting travel times of *pP* and *sP* relative to the travel time of the *P* onsets. Green's functions and the observed waveforms are cross-correlated (WALLACE *et al.*, 1981; ZHAO and HELMBERGER, 1994). This is implemented in a code "teleINV" which uses Green's functions generated by the above teleseismic method and finds the best fitting solution by sweeping through the entire focal parameter space. Figure 1 illustrates an application of this teleseismic modeling using the recent southern India earthquake of May 21, 1997 in Jabalpur of Madhya Pradesh. Depth is particularly well constrained in such teleseismic inversions. The error in depths can be minimized and sometimes depths become resolvable to within ± 1 km using accurate source-region crustal structure (WOODS *et al.*, 1998); even with more general velocity models absolute depth error is likely to be at most ± 5 km (NELSON *et al.*, 1987).

Once the master events' source parameters and locations are determined, their regional records are forward modeled by perturbing the crustal velocity structure to

►

Figure 1

Example of the fit of teleseismic *P* waves used to determine source parameters and depth for an earthquake in India. The observed (thick line) and synthetic (thin line) displacement waveforms have been convolved with a Wood-Anderson long-period instrument. Station name, azimuth and distance, in degrees, are given to the left of the vertical seismograms; the peak amplitude (cm) of each trace is given at the right of each seismogram pair. The synthetic seismograms were computed for the best-fitting focal mechanism solution ($\delta = 65°$, $\lambda = 68°$, $\Phi = 70°$) and event depth of 35 km, shallower than the PDE depth only by 1 km, which were obtained using the grid-search technique. Both vertical and radial *P*-wave seismograms were modeled and only one receiver crust was used for all 27 stations.

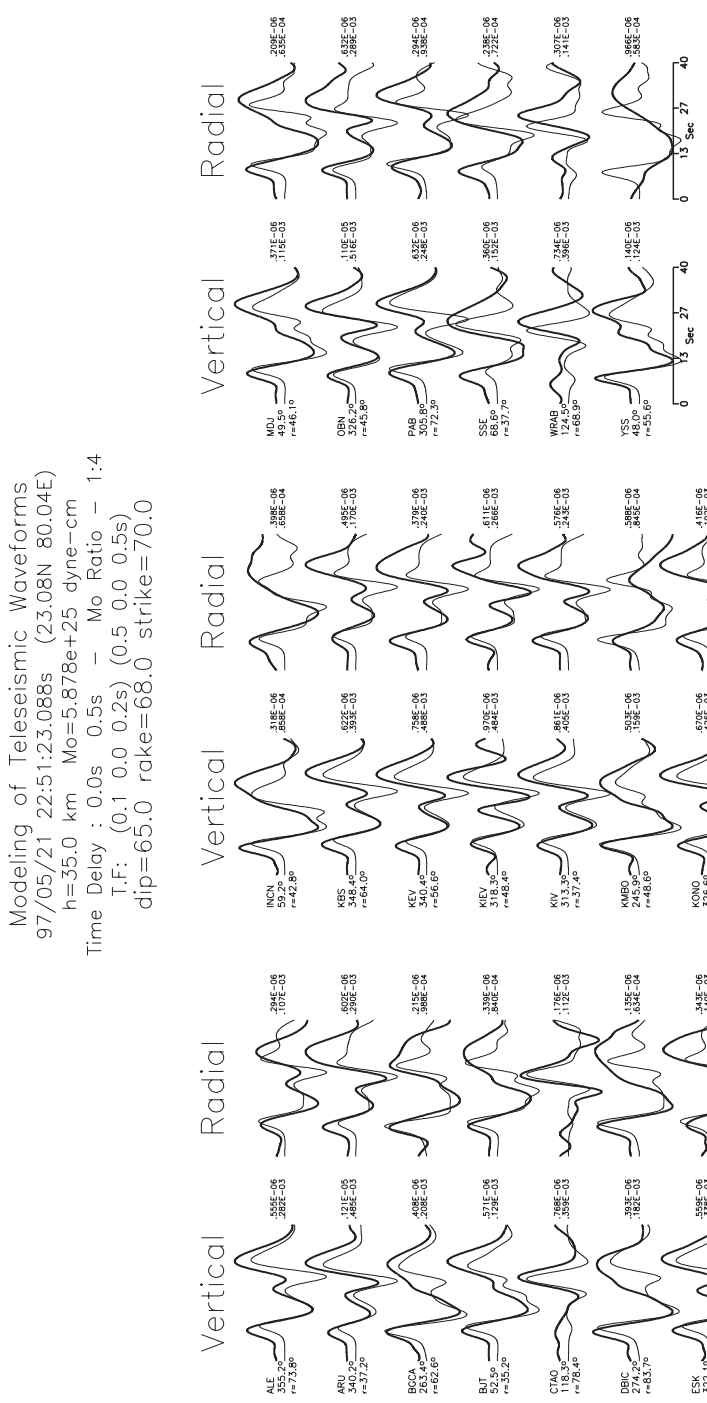
Modeling of Teleseismic Waveforms
97/05/21 22:51:23.088s (23.08N 80.04E)
h=35.0 km Mo=5.878e+25 dyne-cm
Time Delay : 0.0s 0.5s - Mo Ratio - 1:4
T.F: (0.1 0.0 0.2s) (0.5 0.0 0.5s)
dip=65.0 rake=68.0 strike=70.0
Vertical
Radial
Vertical
Radial
Vertical
Radial
ALE 355.2° r=73.8°
ARU 340.2° r=37.2°
BCCA 261.4° r=62.6°
BJT 52.5° r=35.2°
CTAO 118.3° r=78.4°
DBIC 272.2° r=83.7°
ESK 322.1° r=68.3°
GRFO 315.2° r=59.8°
HIA 40.0° r=41.1°
INCN 59.2° r=42.8°
KBS 348.4° r=64.0°
KEV 340.4° r=56.6°
KIEV 318.3° r=48.4°
KIV 313.3° r=37.4°
KMBO 24.5° r=48.6°
KONO 326.6° r=61.1°
LVZ 340.2° r=53.3°
MA2 33.4° r=61.3°
MDJ 49.5° r=46.1°
OBN 326.2° r=45.8°
PAB 305.8° r=72.3°
SSE 68.6° r=37.7°
WRAB 124.5° r=68.9°
YSS 46.0° r=55.6°
0 13 27 40 Sec

better fit the observed waveforms. In conjunction, other geophysical information such as the P_n velocity, Moho depth determined by reflection studies or other methods, teleseismic receiver functions, and surface-wave dispersion data, is used to constrain the model.

The approach taken to develop the regional waveguide is to begin with a relatively simple 1-D model with a couple of crustal layers over a mantle half space; only incorporating additional layers to include the significant discrepancies between observed and synthetic waveforms. Generally this is done by modifying the overall thickness of the crust and velocities of the crustal layers and the upper-most mantle. The primary upper layer, corresponding to the sedimentary structure, strongly affects the Rayleigh waves and the character of the *PL* (extended *P*-wave) and *S* wavetrains (SONG *et al.*, 1996; SAIKIA, 1994; SAIKIA and BURDICK, 1991). If observations suggest a strong gradient in the velocity structure – that is, the initial *P* wave is sharp and impulsive with the character of turning ray rather than the longer period ramp-like head-wave character – a detailed model with a gradient in the mantle structure must be used (SAIKIA, 1994).

Figure 2 is a modeling example showing the agreement between data and synthetic seismograms obtained for a set of three-component regional seismograms from the southern India earthquake, described previously, recorded 645 km away at HYB Hyderabad (HYB), a Geoscope broadband station in India. We employed as an initial regional model one developed by GAUR and PRIESTLEY (1997), using teleseismic receiver function analysis at HYB. The top seismograms are the deconvolved broadband displacement records and the two waveforms immediately below correspond to synthetic seismograms generated using the respective teleseismic and regional mechanism solutions determined by waveform inversion. Both solutions yield similar mechanisms and seismic moment, suggesting a well-constrained stable solution.

Another factor to be accounted for in modeling the crustal waveguide is attenuation, or Q. The amplitude and frequency content of regional seismograms are strongly influenced by the anelasticity of the propagating medium. As attenuation affects absolute amplitudes, it thereby directly affects seismic moment and magnitude estimates. The varying degree of attenuation between NTS and the Russian test sites is found to influence the frequency content of the regional seismograms, thus impacting various regional discriminants (TAYLOR, 1995). As the frequency-wavenumber integration method used to generate the regional Green's functions can directly incorporate the effects of intrinsic Q (SAIKIA, 1994), it can be directly accounted for by forward modeling the absolute amplitudes of the regional waveforms, provided that accurate source information, mechanism and moment, are known – preferably from teleseismic estimates of *P*- and *S*-wave source inversions. With the M_0 and mechanism from the teleseismic data modeling, a trial-and-error approach can be used to best fit the amplitude of various groups of waves in the regional records by modifying the Q values as needed. It is possible that there will be some trade-off between attenuation and source time function, especially more

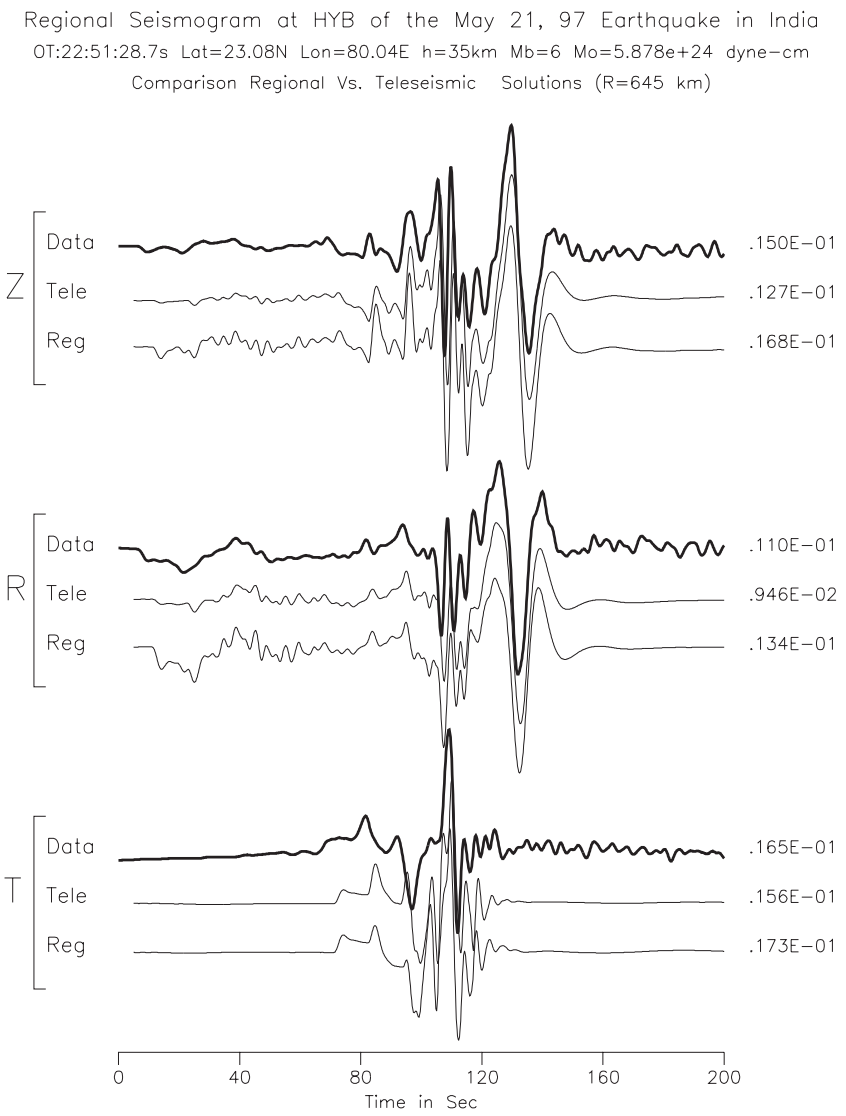

Figure 2

Comparison of observed and synthetic regional seismograms (for the same Indian earthquake shown in Fig. 1); both teleseismic and regional focal mechanism results are shown. The two solutions are similar. A seismic moment of 5.9×10^{24} dyne-cm ($M_w = 5.9$) and depth of 35 km were used. Note the agreement in the amplitude of the P_{nl} waves relative to the surface waves, including the peak amplitudes (cm).

so when the events are large. However, the trade-off can be reduced when both P_{nl} and surface waves are modeled together because the P_{nl} waves attenuate less compared to the short-period surface waves due to the Q effect for the same source function. In an attenuating medium, Q plays an important role in shaping the

frequency content of the surface waves relative to the P_{nl} waves, especially for the shallow events. Of course it is helpful to have a priori Q constraints from other seismological methods or to use as an initial Q model appropriated from other previously studied regions with similar tectonic features. Attenuation related to scattering is best accounted for in regional modeling by developing crustal models for particular paths. In some cases this may be done by simply modifying the Q model for a single crustal model, but often will require the modification of the velocity model as well, sometimes employing thin layers of alternating high and low velocity material in that portion of the waveguide giving rise to the scattering (SAIKIA, 1994).

Regional seismic waves have proven to be amongst the most difficult to analyze or model in deterministic fashion in the field of seismology. At high frequencies the effects of scattering in the crust become so intense that only the statistical properties of waveforms are meaningful. One exception to this generality involves long-period P_n and shear-coupled P (PL) mode body waves at regional distances (1°–12°). HELMBERGER (1972, 1973), and HELMBERGER and ENGEN (1980) have shown these P-wave phases, which comprise the first 1–2 min of the regional wavetrain, to be very stable and straightforward to model with synthetic seismograms. In subsequent studies, WALLACE *et al.* (1981) demonstrated that long-period P_{nl} waveforms are stable and deterministic enough to be utilized in automated inversion schemes to determine source mechanism. LEFEVRE and HELMBERGER (1989) and HOLT and WALLACE (1989) demonstrated that the P_{nl} analysis procedures can be applied without substantial modification to observations from virtually any tectonic region. In a later study SAIKIA and BURDICK (1991) extended the application to shorter period P_{nl} waves and demonstrated that short-period P_{nl} waves also have many stable features which can be deterministically modeled to characterize the regional crustal waveguide. This characteristic of P_{nl} waves is due to their primarily sampling the lower crust and the Moho interface, and consequently being relatively insensitive to lateral crustal variations, which occur mainly in the upper crust. Even for mixed paths traversing continental and oceanic crust in the western Mediterranean, THIO *et al.* (1999) found P_{nl} waveforms to remain quite stable. Hence this portion of the wavetrain can be adequately modeled over long distances with a single model, although its relative timing with respect to the rest of the wavetrain may vary.

Surface waves are also susceptible to lateral variations in the crustal waveguide as they are strongly effected by the lateral variations in the upper crust and mountain topography as well as the moho depth. This is especially true for Rayleigh waves (WOODS and HARKRIDER, 1995; SONG *et al.*, 1996; THIO *et al.*, 1999). Therefore, it becomes difficult to model the entire wavetrain waveform with a single 1-D model. An example of such behavior is provided in Figure 3, taken from THIO *et al.* (1999), which compares the vertical and tangential displacement records for an earthquake in Gafsa in Tunisia (June 12, 1992, origin time: 19 h 16 m 45.7 s) recorded by the stations MEB (Medea, Algeria) and VSL (Villasalto, on the Island of Sardina). The path to MEB is a pure continental one whereas the one to VSL consists of both

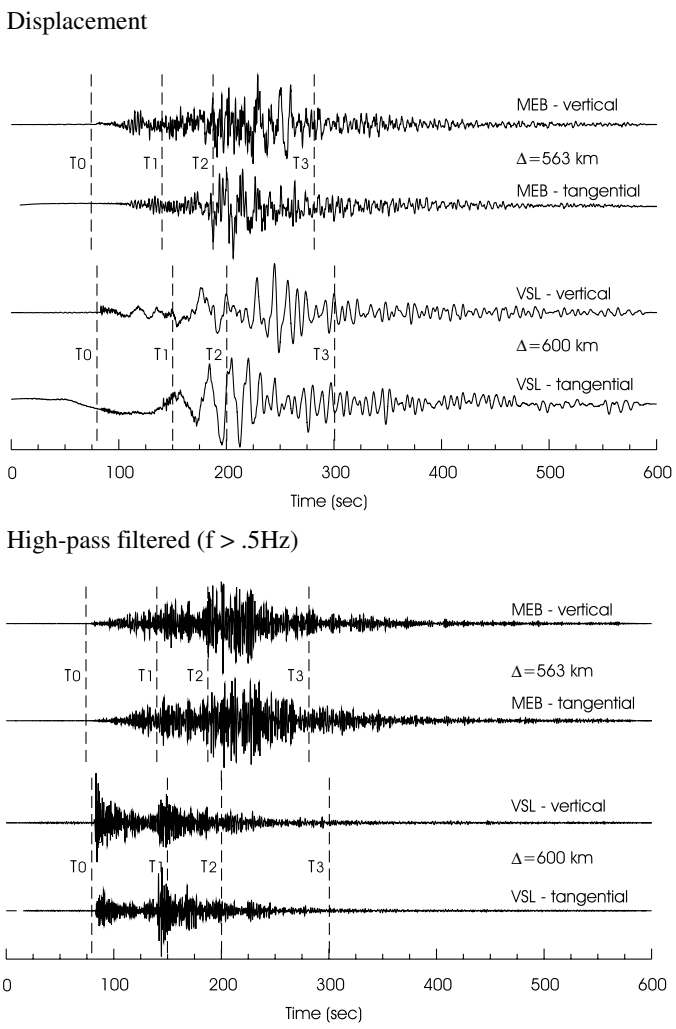

Figure 3

Broadband displacement (upper panel) and high-pass filtered (lower panel) seismograms (vertical and tangential components) for an event in North Africa at Gafsa, Tunisia recorded at MEB and VSL (units are in ''cm''). The path to VSL traverses is the Mediterranean and causes strong Lg wave blockage. The path to MEB is continental. (Notations: the lines **T0**, **T1**, **T2** and **T3** correspond to the travel times for group velocities of 7.5, 4.0, 3.0 and 2.0, respectively.

continental and oceanic sections almost equal in length. The two recordings are at comparable distances, yet the waveforms are very different in character and the surface-wave arrival time is considerably sooner for VSL. A striking feature is found in the frequency content, with the record for the oceanic path to VSL being deficient in high frequencies relative to the one for the pure continental path to MEB.

Another example of the variation in regional waveform propagation characteristics is shown in Figure 4 which compares three pairs of vertical component displacement seismograms, recorded at different azimuths from an earthquake in central Asia. For each pair of seismograms the lower trace is the short-period filtered version of the upper broadband waveform. The top pair of waveforms is for a path crossing the Junggar basin to the station WMQ in China, while the other two seismogram pairs are for paths traversing the Tien Shen mountains to the stations AAK in Kyrgzystan and WUS in China. There is no significant difference in short-period seismograms besides the expected amplitude decay with distance, however the surface waves crossing the basin are modulated to more dispersive ringing signals than are the other two surface-wave observations which, in fact, have longer paths. Generally, more dispersion would be expected from the more distant observations at WUS and AAK, but this is not the case. Modeling these surface-wave observations well with one crustal waveguide is not possible. The use of a crustal model, which consists of a relatively fast upper crust to emulate the effects of the mountain structure recorded at WUS and AAK, to also model the basin effects recorded at WMQ would tend to underestimate the source depth and consequently the seismic moment as well for this observation.

For regions with large lateral variations in crustal waveguide, surface waves are difficult to model using a single 1-D crustal velocity model. One approach to overcome this difficulty is to model the P_{nl} and surface waves separately using a hybrid method in which the surface waves are generated using normal-mode synthesis so that mixed-path synthetics can be produced. A simple and computationally efficient way to account for surface waves traversing a laterally varying structure is by the method of mixed-path synthetics which can account for two or more velocity models along a single path (WOODS and HARKRIDER, 1995; THIO *et al.*, 1999). LEVSHIN (1985) showed that this approximation holds for cases in which $\lambda \gg \ell$, where λ is the horizontal wavelength and ℓ is the scale length of the velocity variation. The cut-and-paste source inversion method (CAP, ZHAO and HELMBERGER, 1992) has the advantage of accommodating P_{nl} and surface-wave Green's functions generated from two or more separate crustal models, including mixed paths (THIO *et al.*, 1999).

Another approach to account for the varying crustal structure along the propagation path is to regionalize the phase velocity model to correct for the surface-

►

Figure 4

(a) Map showing the location of event 96072 and the three recording stations: AAK, WMQ, and WUS, (b) vertical component displacement records for event 96072. Three pairs of traces are shown, the top one corresponds to the recorded broadband displacement and the lower one to the Wood-Anderson short-period instrument play-out (units are in "cm"). Note the strong dispersive ringing character of the WMQ displacement record, which traverses primarily basin structure, compared to the other two observations which traverse the Tien Shen mountains.

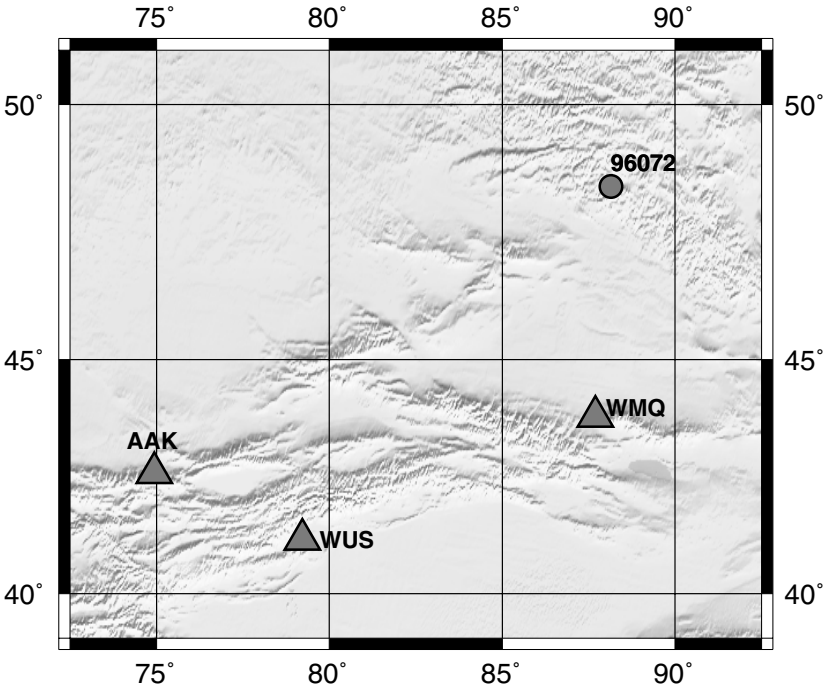
75˚
80˚
85˚
90˚
50˚
45˚
40˚
96072
WMQ
AAK
WUS

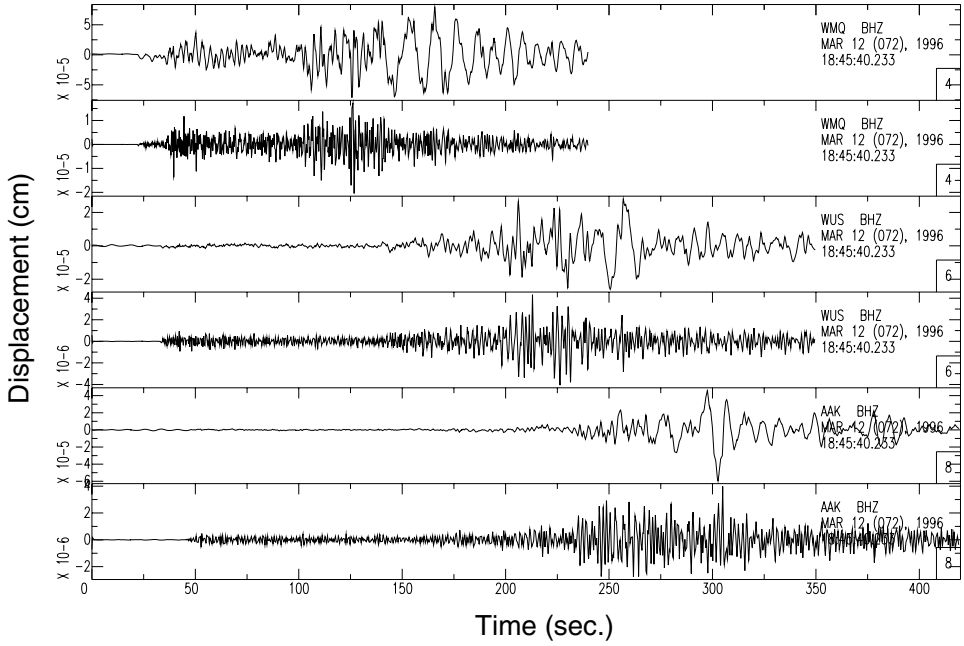
Displacement (cm)
Time (sec.)
WMQ BHZ
MAR 12 (072), 1996
18:45:40.233
WUS BHZ
MAR 12 (072), 1996
18:45:40.233
AAK BHZ
MAR 12 (072), 1996
18:45:40.233
X 10-5
X 10-6

wave path effects. This method is based on the fact that to a first-order perturbation in structure to a homogeneous velocity model is primarily in the phase velocity and is widely used in the surface-wave studies (DZIEWONSKI and STEIM, 1982; NAKANISHI and KANAMORI, 1982). THIO and KANAMORI (1995) applied successfully a regionalized phase velocity model for moment tensor inversion in southern California using short-period (10–60 s) surface-wave data. One drawback to this method is that, unlike the method used by WOODS and HARKRIDER (1995), it does not account for the amplitude changes that can occur when surface waves propagate from one medium to an adjacent one with varying crustal waveguide properties. However, it provides a means to adequately model surface waves in regions of strong lateral variations. Figure 5 shows a suite of synthetic seismograms generated using the approach of THIO *et al.* (1999) in which Rayleigh waves have been generated for a suite of mixed paths, starting with a purely Spanish (continental) path and sequencing through a range of mixed paths with increasing contributions from the Mediterranean (oceanic) path, to a purely Mediterranean path. The panel to the right displays the models. The change in the composition of the mixed-path model clearly has a strong influence on the arrival times as well as on the waveforms. An application of this approach to surface wave modeling is shown in Figure 6, which compares observed and synthetic waveforms at four stations, MEB, VSL, TAM and

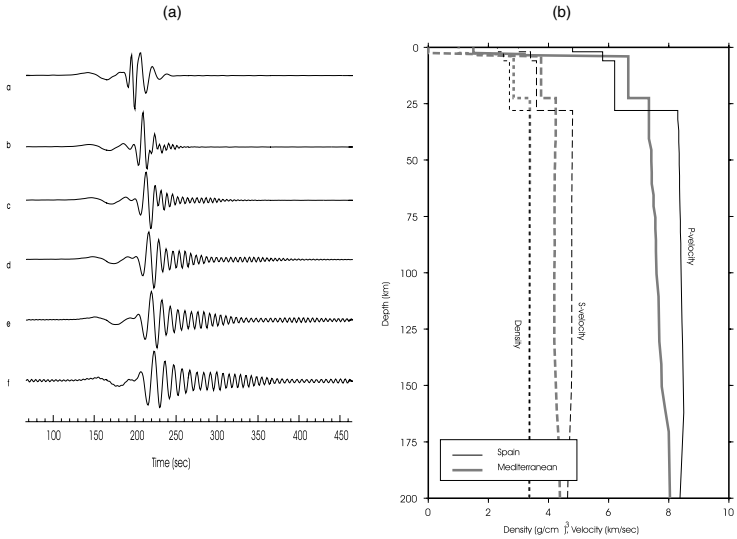

Figure 5
(a) Vertical-component Rayleigh waves simulated using the mixed-path approach for differing ratios of purely continental (Spanish model) and purely oceanic (Mediterranean model) paths: i) 100% Spain path, ii) 80% Spanish/20% Mediterranean, iii) 60%/40%, iv) 40%/60%, v) 20%/80%, and vi) 100% Mediterranean path. (b) Regionalized velocity models used to generate the hybrid surface-wave synthetics shown in Figure (a).

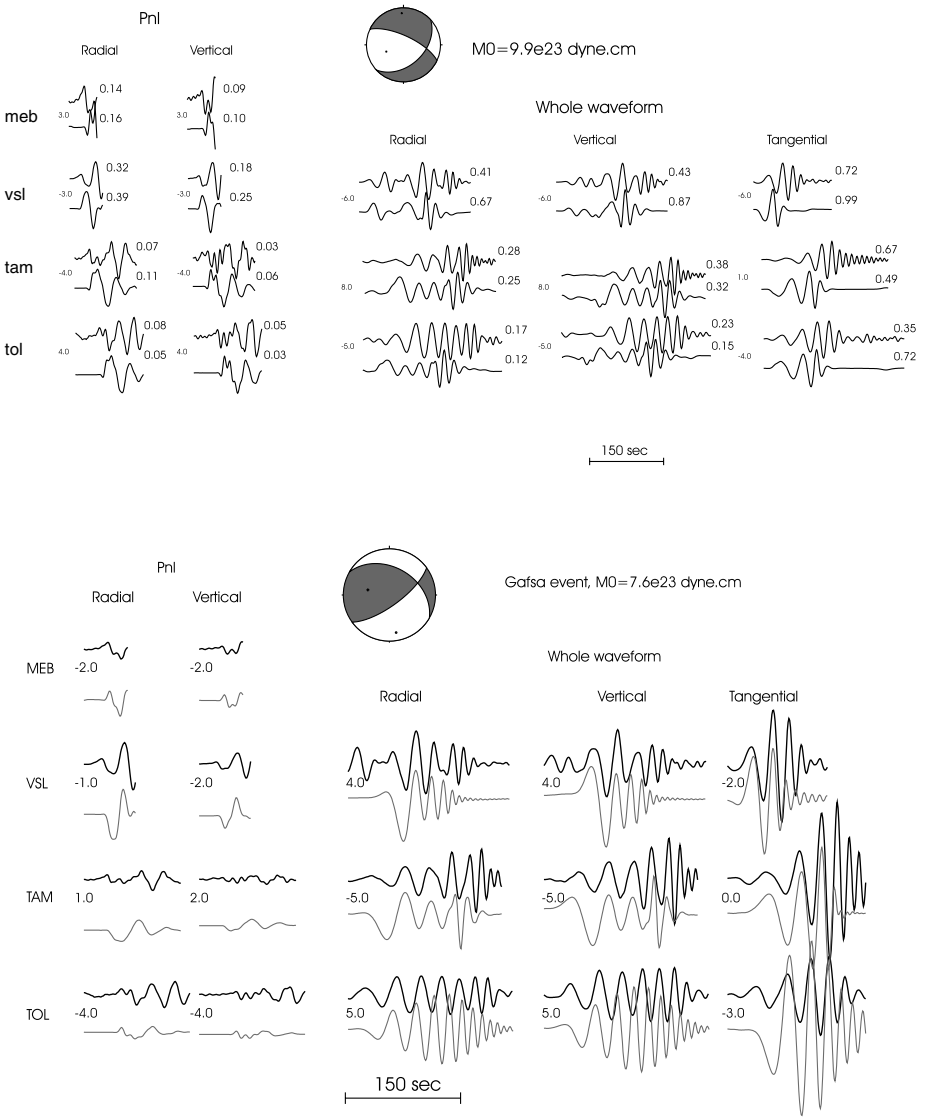

Figure 6

Source inversion results for the Gafsa, Tunisia earthquake (6/12/92). (a) Results using a single 1-D model. The top trace in each pair is the observed waveform; the lower trace is the synthetic. The time shift between the two seismograms is printed to the left of each pair, with a positive number indicating a fast synthetic; peak amplitudes (cm) given to the right of each trace. (b) Source parameter solution for the same event using mixed-path (continental and oceanic crust portions) synthetics for the surface waves; P_{nl}-wave synthetics were computed using a single 37 km thick crust.

TOL, for an earthquake which occurred on June 12, 1992 (19 h 16 m 45.7 s, $M_w = 5.2$) near Gafsa, Tunisia, in North Africa. The top panel displays inversion results using a single 1-D model for all stations, with peak amplitudes given to the right of each trace and the observed waveform above the synthetic in each seismogram pair. These results exhibit inconsistencies in waveform fitting. The mechanism solution is also inconsistent with the Harvard CMT as well as with that of the moment tensor solution obtained from mixed-path surface-wave inversion, results of which are presented in the panel below. It is clear that one 1-D model cannot even fit the surface wave data even with a longer period, whereas the mixed-path synthetics yield satisfactory results. The lower panel displays the results of the mixed-path synthetics for the surface waves (the P_{nl} wavetrain was modeled with a single 1-D model). The waveform fits are significantly better and the source mechanism is consistent with the Harvard CMT solution.

Once the crustal waveguide model is established for a region or province, it can be used to locate events and to estimate their source parameters from waveform inversion. This event analysis of regional seismograms can be routinely applied to smaller events ($4 \leq M_w \leq 5$) for which teleseismic observations are too small to be analyzed.

Source Inversion Methodology Using Regional Seismograms

In this section we present a brief summary of a methodology for inverting regional seismograms. We discuss the effectiveness of the method by comparing results obtained by inverting regional seismograms from two stations versus regional seismograms from two full networks consisting of multiple stations with a better azimuthal coverage. The mathematical details have appeared in several other publications (ZHAO and HELMBERGER, 1994; ZHU and HELMBERGER, 1996) therefore we shall only discuss the salient features of this source inversion method.

There are two issues which make it difficult to use the entire seismogram for source estimation. First, the whole-seismogram inversion is mainly controlled by the surface waves because of their large amplitude relative to that of P waves, except in the case of deep events. However the P waves, especially the long-period P_{nl} waves, are very useful for source estimation as they are stable and insensitive to variations in the velocity structure (HELMBERGER and ENGEN, 1980; SAIKIA and BURDICK, 1991). Further, the amplitude ratio between the P_{nl} and surface waves is a good indicator of source depth, consequently both wavetrains should be properly weighted in the inversion. Secondly, as these two parts of the wavefield propagate through different portions of the regional waveguide, the crustal velocity model must be able to accommodate these effects.

Waveforms at regional distances are generally complex due to propagation effects and the source rupture processes, especially in the case of larger events. Because of

the path effects alone it is often difficult to fit the relative timings between the P_{nl}, S_{nl} and surface waves, especially in regions known to contain laterally varying crustal structure; fitting the relative timing between the Rayleigh and Love waves can also be quite difficult. Therefore, to invert regional waveform data, ZHAO and HELMBERGER (1994) developed an approach in which the P_{nl} and surface waves are split into two separate wave groups in order to mitigate timing differences between the two wavetrains in the synthetic and observed seismograms. This approach is popularly known as the cut-and-paste (CAP) method, which allows the fitting of the P_{nl} and surface-wave waveforms together while disregarding their relative timings. A similar approach was also applied by SAIKIA and HERRMANN (1985) for inverting local seismograms in which they separated the P seismograms from the S seismograms to obtain focal mechanisms and event depths. The CAP approach makes the source inversion relatively insensitive to the velocity model and lateral crustal variations as well as proving quite useful when the initial event locations are poorly constrained. However, as the waveform misfit errors are normalized by the data and synthetics, the amplitude information of the data is not fully utilized to constrain the source orientation and event depth.

To fully utilize the amplitude information, ZHU and HELMBERGER (1996) used a distance scaling factor to normalize amplitudes in the inversion, to avoid bias in the estimated source parameters introduced by the nearer observations. Both P_{nl} and surface waves are normalized to a reference distance r_0 allowing the P_{nl} waves to decay as $1/r$ and surface waves as $1/r^{1/2}$. A general expression for the misfit error e between a segment of observed $u(t)$ and synthetic $s(t)$ waveform is given by

$$e = (r/r_0)^p ||u(t) - s(t)|| \ ,$$

where the scaling factor p is 1 for the P_{nl} waves and 0.5 for the surface waves. These scaling factors may be adjusted corresponding to the actual amplitude decay rate of these waves after a certain amount of data has been accumulated for a particular area. For the whole waveform the total misfit error is a weighted sum of the two errors estimated for the P_{nl} and surface waves using the above expression. Surface waves, in general, show larger waveform misfits compared to those of body waves as the surface waves are more affected by lateral heterogeneity in the crustal waveguide, whereas P_{nl} waves are relatively insensitive to structural variations. However since surface waves from an earthquake are generally larger in amplitude, by a factor of 2–4, the inversion can be weighted more heavily for the P_{nl} waves to improve the source estimate. Because of this scaling, the relative P_{nl} and surface wave amplitude information of stations at extended distances is also preserved.

As in the teleseismic inversion, the regional source inversion applies a grid search through the focal mechanism parameter space for a suite of depths, and the synthetic and observed seismograms are cross-correlated for the best alignment (WALLACE *et al.*, 1981; DREGER and HELMBERGER, 1993). For many crustal earthquakes which are recorded by only one or two regional stations and are too small to be recorded at

teleseismic distances with good signal to noise ratios, their depths are poorly constrained by current location procedures. Therefore, for these types of events it is necessary to have reliability checks on these locations that are obtained using only a few observations. Previous studies in the Hindu-Kush region of the Pamir Himalaya have shown that it is possible to obtain reliable depth estimates for such earthquakes using only a few regional observations (SAIKIA *et al.*, 1996a, b; ZHU *et al.*, 1997). Figure 7 provides examples of source depth vs. error curves for earthquakes in this region, which illustrates that depths determined from regional waveform inversion of two stations (dashed lines) are similar to those using many stations (solid lines). The left panel presents results for five shallow earthquakes, while the right panel is for five deep earthquakes. The observations used in the source inversion were taken from PAKN (a PASSCAL network consisting of 11 broadband stations which operated in Pakistan near Nilore, NIL towards its northeast in 1992) and KNET (a permanent array in Kyrgyzstan) networks. The two-station inversion used one station from each of the networks. For the shallow crustal earthquakes, solutions are stable over a broad range of depths and have well resolved waveform misfit errors. The two inversions (two station vs. two networks) yielded similar source depths for all events. These focal depths are notably shallower than their depths given in the ISC bulletin. Figure 8 compares observed and synthetic waveforms for two earthquakes, one shallow and one deep, from 10 earthquakes studied in Figure 7. The agreement in these waveforms suggests that the regional depth solutions are reliable.

To establish the reliability of the regionally determined depth estimates, teleseismic *P*-wave seismograms from these events, taken from the short-period array, were examined for their *P*, *pP* and *sP* phases. The teleseismic short-period array seismograms clearly exhibit depth phases, especially when the seismograms are stacked. Figure 9 presents examples of short-period array data recorded at Alice Springs (ASP) and Waurramunga (WRA) in Australia, Chiang Mai (CHG) in Thailand, and Gauribidanur (GBA) in India for a Hindu-Kush earthquake of (date: 11/19/92, origin time: 02 h 38 m 50.1 s) along with a suite of synthetic seismograms for various depths; the best-matching synthetics are for a 10 km source depth, which is consistent with that determined from regional waveform modeling. Similar agreement was found for the other events so analyzed. The fact that the regional source inversion yields a depth compatible to the observations for four teleseismic arrays, establishes the strength of this source inversion method. As even with stacked array data, the teleseismic observation magnitude (M_w) threshold is about 4.2, thus the regional modeling may be quite useful for smaller events.

Depth Resolution Based on Regional and Teleseismic Depth Phases

The depth of an earthquake is a critical source parameter for the path calibration purposes as it helps to constrain the epicenter and obtain reliable origin times.

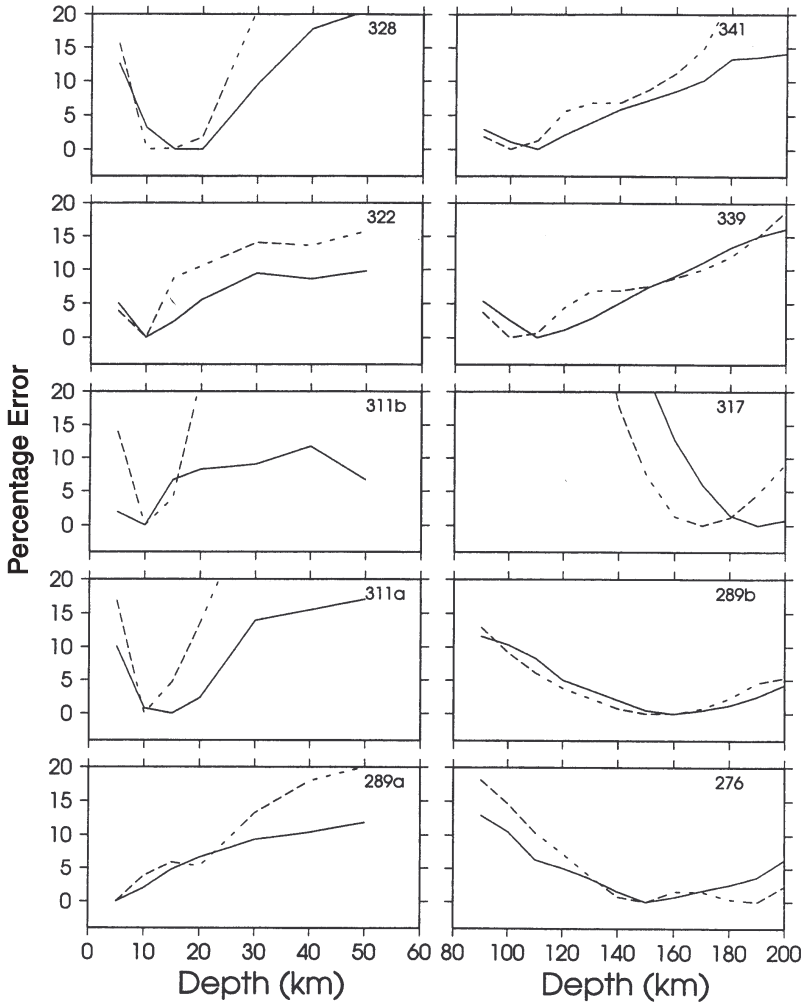

Figure 7
Waveform misfit error as a function of focal depth for 10 Hindu-Kush earthquakes. Solid lines correspond to the misfit error when the solutions were obtained using all seismograms from both PAKN and KNET networks and dashed lines correspond to the solutions when only one station from each network was used (taken from SAIKIA *et al.*, 1996; ZHU *et al.*, 1997). Note that the two minima for each event occur at the same depth.

Criteria adopted for the selection of the ground-truth catalog must be based on the reduced level of uncertainty as discussed by ENGDAHL (1998). However, earthquakes occur in regions where many of those criteria are not met, especially for depth and origin times. If depths are not known and regional crustal models are not adequate, events can be mislocated significantly away from their true locations. In general, the

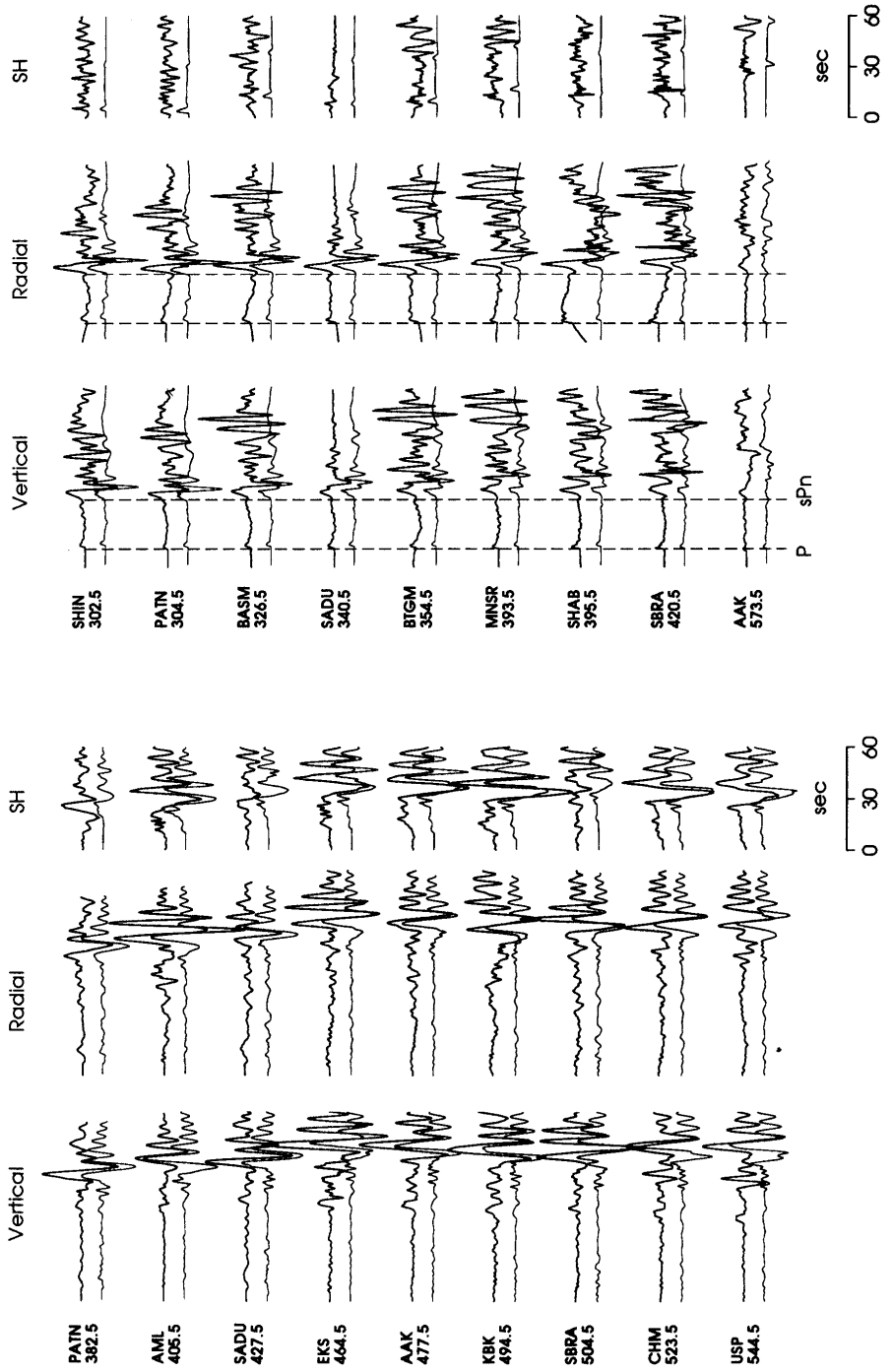
Vertical
Radial
SH
PATN 382.5
AML 406.5
SADU 427.5
EKS 464.5
AAK 477.5
KBK 494.5
SBRA 504.5
CHM 523.5
USP 544.5
SHIN 302.5
PATN 304.5
BASM 326.5
SADU 340.5
BTGM 354.5
MNSR 393.5
SHAB 395.5
SBRA 420.5
AAK 573.5
P
sPn
sec
0
30
60

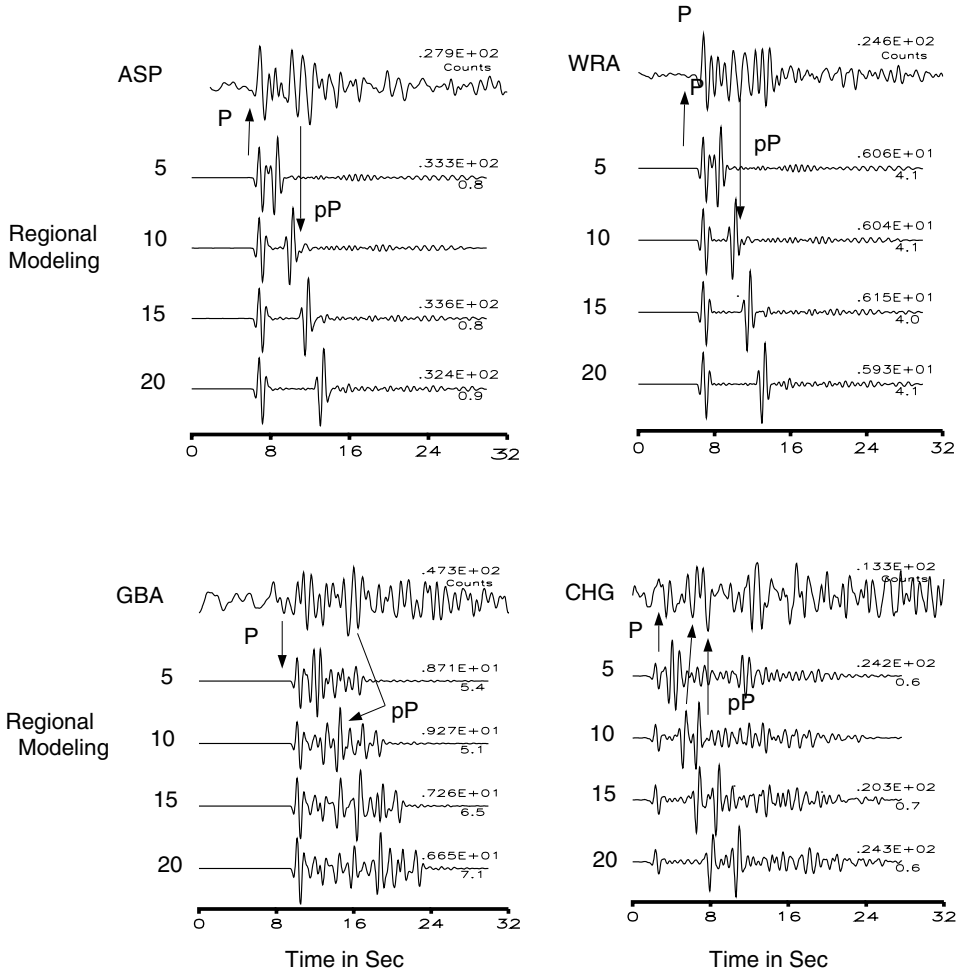

Figure 9

Modeling of the P-wave depth phases for a Hindu-Kush earthquake (Nov. 17, 1992; origin time-02 h 38 m 50.1 s; $M_0 = 1.41 \times 10^{23}$ dyne-cm) observed at four short-period teleseismic arrays: Alice Springs (ASP) and Warramunga (WRA) in Australia, Gauribidanur (GBA) in India, and Chiang Mai (CHG) in Thailand. In each panel the top seismogram is the observation; below this is a suite of synthetic seismograms at depths ranging from 5 to 20 km using its regional focal mechanism solutions. Synthetics computed for a depth of 10 km clearly produce the best fit to the recorded *pP* phase relative to the *P* waves; this was the depth determined from regionally modeling as well.

◀

Figure 8

Regional waveform fits for two Hindu-Kush events (taken from SAIKIA *et al.*, 1997; ZHU *et al.*, 1997), one shallow (left: $\delta = 45°$, $\lambda = -35°$, $\Phi = 200°$, and $h = 15$ km) and one deep (right: $\delta = 35°$, $\lambda = -55°$, $\Phi = 290°$, and $h = 110$ km), shown at several stations from the PAKN and KNET networks. For each station the synthetic seismogram is plotted immediately below the observed seismogram; displacement is in "cm". Synthetic seismograms were computed using the frequency-wavenumber integration algorithm (SAIKIA, 1994).

depths of earthquakes reported in various catalogs are biased (ZHAO and HELMBERGER, 1991a; ZHU *et al.*, 1997; SAIKIA *et al.*, 1996a, b; THIO *et al.*, 1999) because of the errors in travel-time picks of the *P* and *S* phases, inappropriate crustal models used for locating events, and misidentification of the depth phases (*sP* or *pP*).

Figure 10 depicts relocation of sixty moderate-sized Tibetan earthquakes (ZHAO and HELMBERGER, 1991a); the top panel shows a map view of the earthquakes investigated, the middle panel shows the cross-sectional view of the depths of the relocated earthquakes and the bottom panel shows the ISC depths for the same earthquakes. The new depths were estimated by modeling waveforms of teleseismic depth phases. It is interesting to note that all events have moved to shallower depths relative to the ISC depths except for one event. Errors in location result primarily from errors in the estimation of depths, especially for shallow earthquakes and also from the lack of regional models. ZHU and HELMBERGER (1996) observed similar variation changes in source depths in southern California wherein regional waveform inversion yielded deeper focal depths than the local network's. It has been argued that the *P*-wave model used by the local network is too fast and thus forces the earthquakes to shallower depths (DI LUCCIO *et al.*, 1998). Thus regional broadband waveform modeling and source inversion can provide more accurate hypocentral locations than those from extensive local networks, which hitherto were thought to provide the most reliable results.

We present similar results, in Figure 11, for twenty seven Hindu-Kush earthquakes whose depths were estimated by minimizing the misfit between the observed and synthetic regional waveform using regional seismograms from the PAKN and KNET networks, and the station NIL in Pakistan. The regional depths are marked by blue circles which were also confirmed by a separate waveform modeling of the teleseismic depth phases (SAIKIA *et al.*, 1996a). The corresponding ISC Harvard CMT depths are designated by red circles. The top panel shows the relative depths for the events which have ISC depths larger than 90 km. These events were relocated with respect to their epicentral location by first constraining their depths to the regional-waveform inverted values, and then applying an adaptive grid-location scheme to search for the best epicentral location over a 1° by 1° area, centered about the ISC location, by minimizing the travel-time residuals for each event (ZHU *et al.*, 1997; SAIKIA *et al.*, 1996a). We relocate these events by minimizing regional travel-time residuals of the *P* and *S* waves for the fixed source depth using the object function defined by

$$\mathbf{\Phi}(x,y) = \sqrt{\frac{1}{N}\sum_{i=1}^{N}(\delta T_i - \overline{\delta T})^2} + \lambda \mathbf{\Delta} r \ ,$$

where x and y are the horizontal coordinates and δT_i is the travel-time residual of a first *P* or *S* arrival at station *i*. The average residual over all stations, δT_{ave}, is subtracted to remove the uncertainty of origin time; Δr is the offset between the new and the original location and the weighting constant λ is set to 0.01 s km^{-1}. This

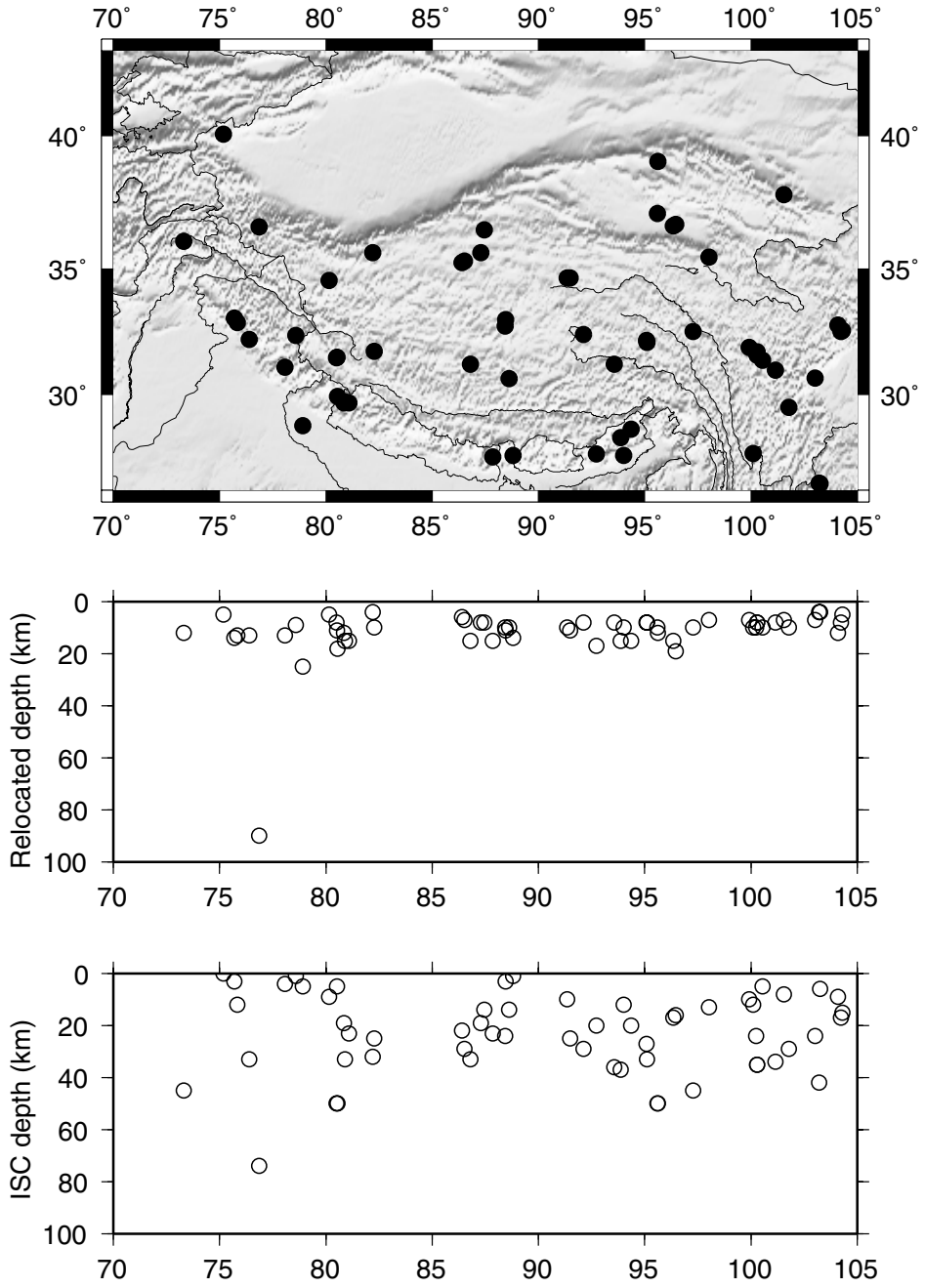

Figure 10
Relocation of 60 earthquakes in Tibet (taken from ZHAO and HELMBERGER, 1991). Top panel shows the epicentral locations of these events. The bottom and middle panels show the ISC and the corresponding relocated depths of these events, respectively. Note that, except for one event, all events moved to shallower depths.

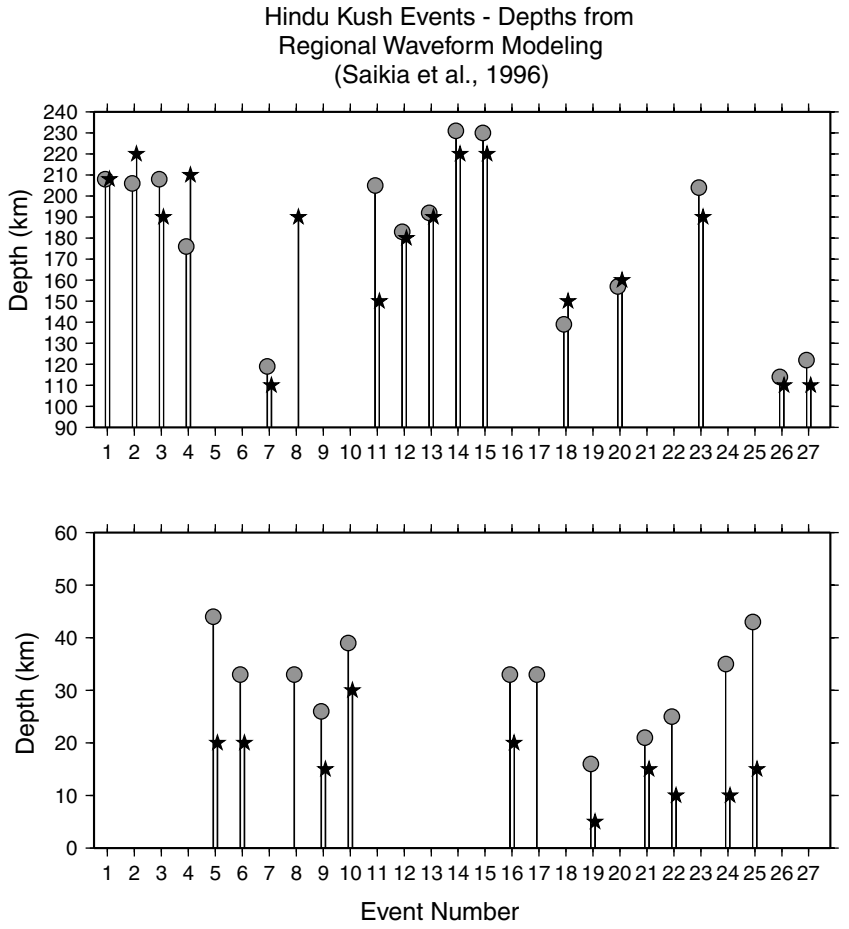

Figure 11
Depths determined by modeling regional waveforms (black stars) recorded at NIL (Nilore) and SBRA (surrogate station for NIL) in Pakistan and AAK in Kyrgyzstan are compared to depths reported in the ISC bulletin (grey circles). All crustal events (lower panel) have moved to shallower depths. These events were relocated using the adaptive grid-search technique (ZHU *et al.*, 1997; SAIKIA *et al.*, 1997) by constraining their depths to the regional solutions; for events which are small ($M_w \leq 4.2$) the new epicenters shifted by more than 30 km relative to the ISC locations.

algorithm was also extended to many smaller ($M_w < 4$) events using regional seismograms recorded by the PAKN and KNET network and applying the same regional crustal model (SAIKIA *et al.*, 1997). We found, in general, that the locations of smaller events moved the most relative to the ISC solutions – up to 30 km in some cases. Table 9 in SAIKIA *et al.* (1996a) summarizes the locations of several Hindu-Kush events determined using *P*- and *S*-wave travel times and waveform modeling of the PAKN and KNET network seismograms with those of the ISC and AFTAC (Air

Force Technical Application Center) locations. The table gives the locations determined using distant *P*-wave travel-times (teleseismic), locations using *P*- and *S*-wave travel times from the PAKN and KNET network stations for both free and fixed depths (local and local fixed-depth locations, respectively). For fixed-depth locations, depths were constrained to the depths estimated by the waveform modeling. For these events, locations determined by applying the adaptive-grid search technique by minimizing the travel-time residuals using travel-time data only from two stations, and constraining the depths to the waveform-modeling depths, were found to be similar to those locations determined using the local *P* and *S* travel times for fixed depths using travel-time data from all stations of the PAKN and KNET networks. In this paper we summarize the results of Table 9 of SAIKIA *et al.* (1996a) in Figure 12 (for details refer to the figure caption).

Mislocation of source depth has also been encountered with events occurring in central Asia (WOODS *et al.*, 1998), and Egypt (THIO *et al.*, 1999). Figure 13a compares depth estimates for 26 central Asian earthquakes, determined by WOODS *et al.* (1998) using regional broadband waveform inversion of P_{nl} and surface waves (purple circles) and teleseismic *P*-wave modeling (light blue), with those of PATTON (1998), who used regional surface wave spectral inversion (green, Patton), and with Harvard CMT (dark blue) and PDE (red) catalog values. Although the depth estimates are quite consistent between all methods for 8 of the events (#'s 6, 8, 9, 11, 18, 19, 23 and 25), there is considerable variation in the other events, with the Harvard CMT or PDE depth generally being the greatest. However, the depths determined by the inversion of regional P_{nl} and surface waves (yellow), and by modeling of the teleseismic depth phases (red) are quite consistent, with relative differences of less than 10 km, suggesting validation of the two sets of results. Some of the spectral depths (green, Patton) are particularly shallow relative to the other results.

Source depth not only can trade off with origin time but can also effect the epicentral locations. An example of this is shown in Figure 13b, which indicates the results of relocating 17 of the above 26 central Asian earthquakes by Aaron Velasco (personal communication, Los Alamos National Laboratory, 1998) using regional and teleseismic travel-time data and a velocity model of MOONEY and LI (1997) for the region. The upper panel shows the fixed (constrained to the average value of WOODS *et al.*, 1998) and free depths for the relocations and the bottom panel plots the shift in epicentral distance, ΔR, relative to the EDR locations for the fixed-depth and unconstrained hypocentral locations. Some events, for example events 7 and 16, moved significantly away from the EDR locations for the unconstrained hypocenter relocations. Assuming the EDR locations are accurate, then the constrained-depth relocations are more accurate. In either case, the location of an earthquake will trade-off with how well its depth is determined or constrained. In general, depth is the least controlled parameter and establishing its ground-truth value is essential for accurate epicentral locations.

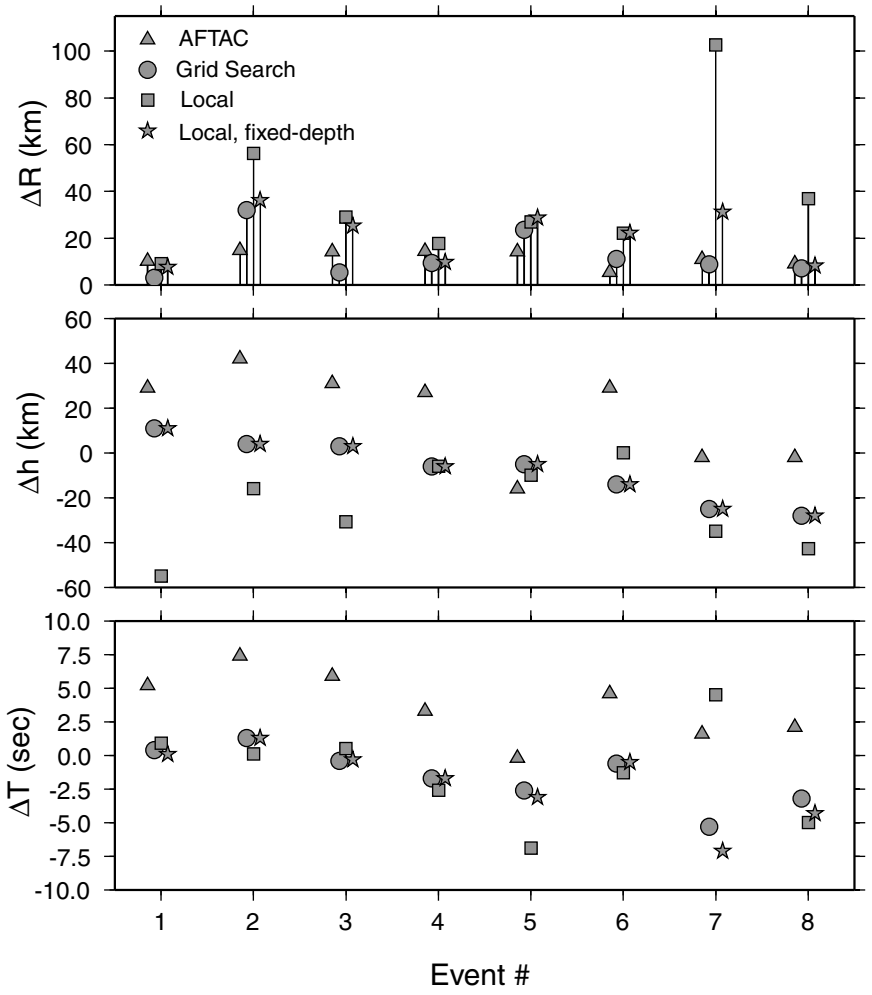

Figure 12
Comparison of various location results for 8 Hindu-Kush earthquakes; all values are relative to the ISC values. Local (squares) and local fixed-depth (stars) locations were obtained by using *P*- and *S*-waves travel-time data from the PAKN and KNET networks. For local fixed-depth locations depths were constrained to the regional waveform modeling depths (SAIKIA *et al.*, 1996). Grid search locations (circles) were obtained using travel-times from the PAKN and KNET networks for a minimum required number of stations applying the adaptive grid-search technique, and triangles correspond to the locations provided by AFTAC. *Top*: relative shift (Δr) in epicentral locations; *Middle*: relative shift in depth (Δh), with negative values indicating a shallower depth than the ISC value; *Bottom*: difference in origin time (ΔT), with a negative value indicating an origin time earlier than the ISC value. Note the similarity between the results for the local fixed-depth and the grid-search locations.

For crustal earthquakes, the ratio of the P_{nl} wave amplitude relative to the surface wave amplitude is diagnostic of source depth, as shallow earthquakes generate larger amplitude surface waves whereas the primary body-wave phases tend to be sharper

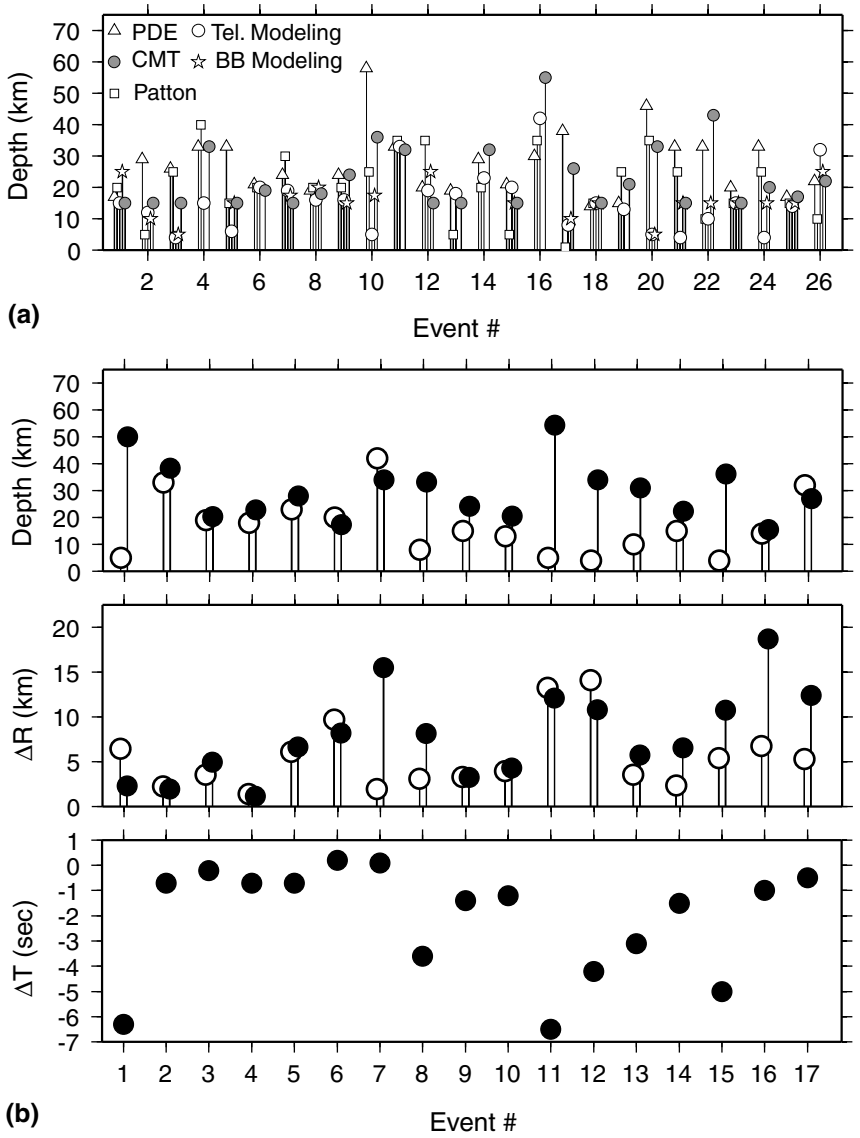

Figure 13

(a) Comparison of source depths, determined by five different methods, for 26 central Asian earthquakes: PDE values determined from teleseismic *P*-wave first arrivals (triangles), Harvard CMT solutions (filled circles), PATTON's (1998) solutions using regional surface wave spectra (squares), and teleseismic *P*-wave waveform modeling (open circles) and BB regional waveform modeling (stars) results from WOODS *et al.* (1998). Generally the PDE depths, which are similar to ISC values, yield the deepest focal depths. (b) Of these events, seventeen were relocated using regional and teleseismic travel times and a regional crustal model. This was done for two cases, one for unconstrained depths (filled circles) and one whereby the depth was fixed (open circles), based on regional and teleseismic modeling. The top panel is a plot of the two sets of depths; the middle panel shows the relative shifts of epicenters from the EDR epicenters after relocations using fixed and free depths; and the bottom panel gives the relative origin times ($T_{\text{fixed}}-T_{\text{free}}$).

and larger in amplitude as source depth increases. For crustal earthquakes, interaction of the *sPmP* phase, which leaves the source as a *S* wave and is converted to a *P* wave at the free surface before being reflected at the Moho boundary with the *PmP* and *Pn* phases, is also a good indicator of depth (SAIKIA and HELMBERGER, 1993). In addition, as the earthquakes move into the mantle, the high-frequency waves trapped by the crustal waveguide begin to disappear and the primary body wave phases become dominant, thus making the seismograms increasingly simple for deeper – particularly mantle – earthquakes (SAIKIA *et al.*, 1996b). Generally, for deep events a strong long-period phase (*sPn*) appears on regional seismograms as shown by the dashed line in Figure 14, which is diagnostic of deep mantle earthquakes. The seismograms shown in this figure were recorded by the PAKN and KNET networks. The phase *sPn*, shown in Figure 14, follows an *S*-wave path to the surface and becomes critical developing a head wave by *S*-to-*P* mode change. It begins slowly at large on the PAKN network and has a sharper onset on the KNET at similar distances see top panels). The detailed characteristic of this phase is controlled by the crustal waveguide. This phase is less impulsive at PAKN because there exists a sharp crust-to-mantle transition with uniform velocities. Beneath KNET there exists a more gradual crust-to-mantle transition zone along with a mantle gradient which causes *sPn* to be sharp. This long-period feature is quite stable and, given its broadband nature jointly with that of *sPmP*, is more important than the direct *S* waves for source depth estimation. Recently a number of studies have investigated this phase in order to constrain event depth (SINGH *et al.*, 1995; LANGSTON, 1996; ZANDT *et al.*, 1996). However, it can also suffer from *S*-to-*P* interaction at the bounce point causing potential ambiguity in its use for source depth analysis. Since this *sPn* phase is a long-period phenomenon, its diagnostic strength in source depth estimation is, perhaps, limited to only larger ($M_w \geq 5$) events.

The interaction of *sPmP* with *PmP* and *pPmP* phases can also be useful in constraining depths for crustal earthquakes. Figure 15 illustrates an example of this interaction observed in regional data, which is also well simulated synthetically both in the broadband data (left) and in the long-period (Press-Ewing 30–90) simulation (right). This earthquake, which occurred on March 25, 1990 (origin time: 17 h 28 m 26.8 s), was recorded at the station GARM, in the former Soviet Union. The small arrows highlight the various phases which are well constrained and correlate well with the data. The first arrow in the broadband seismograms indicates the initial *Pn* phase and the second arrow in the radial broadband seismograms (left panel) shows the arrival of *PmP*. The third arrow shows a strong depth phase which is the *sPmP*. Figure 16 illustrates the critical aspects of the *sPmP* interaction with the *PmP* phase as a function of source depth. The synthetic vertical and radial components are computed for the *PmP*, *PmP* + *pPmP* and *PmP* + *pPmP* + *sPmP* phases at a distance of 345 km and at an azimuth of 312° (panel a). They are generated using the Garm region crustal model; a source mechanism of strike = 60°, dip = 50°, and rake = −165°, and a source depth of 15 km. These same seismograms are convolved

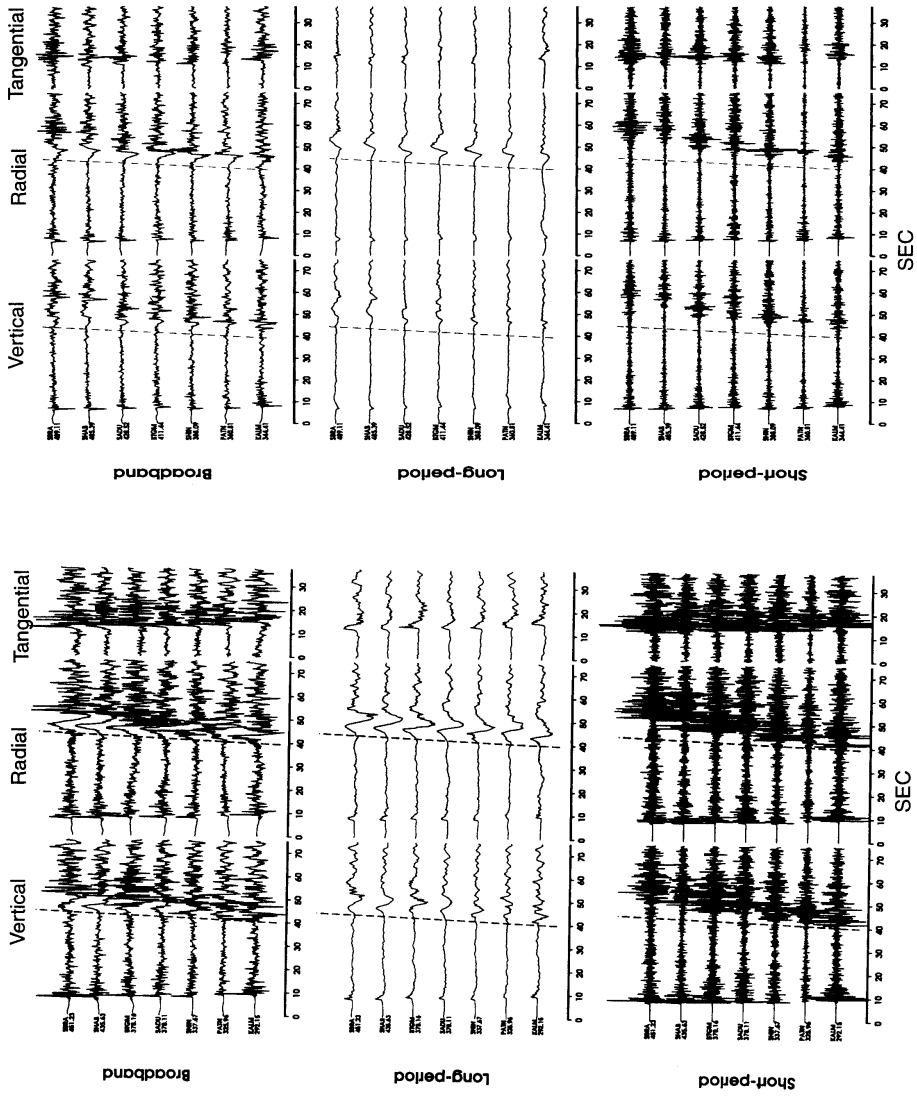

Figure 14
Seismograms from the PAKN (left) and KNET (right) networks for a Hindu-Kush event of Oct. 15, 1992 (OT: 19 h 42 m 13.8 s) which has a depth of 157 km (ISC). The top, middle and bottom panels are the broadband, long-period and short-period seismograms for a window of 30 seconds, respectively. The dashed line is the *sPn* phase, a phase that follows *S* waves to the free-surface, becomes critical and changes to *P* mode. This is a long-period feature which does not appear in short-period data, and is a diagnostic of deep events.

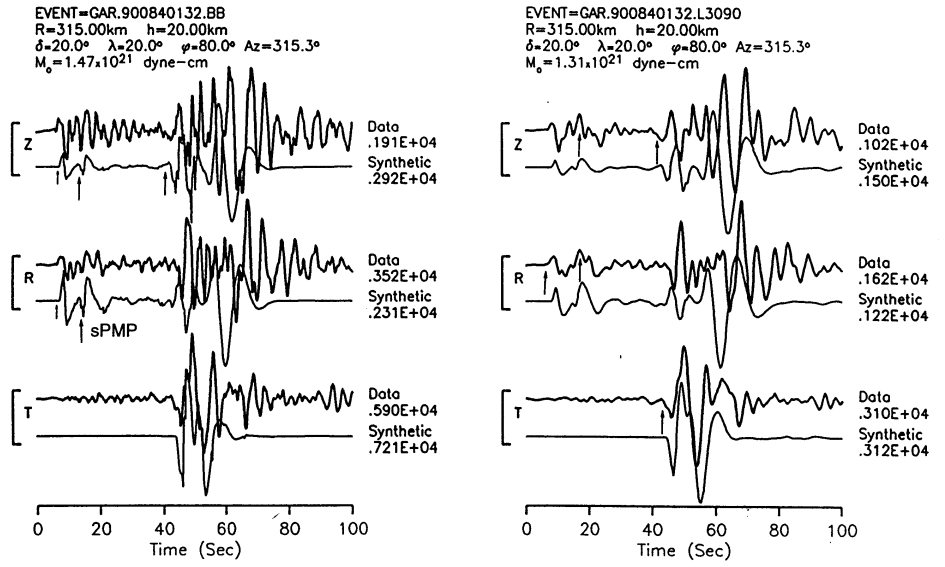

Figure 15
Modeling of regional seismograms from a Hindu-Kush event (900841728) recorded at GARM station. The figure shows the interaction of the *sPmP* and *pPmP* depth phases with *PmP*. The Press-Ewing LP3090 seismograms are simulated by convolving the recorded waveforms with the response of the instrument. For each component the synthetic seismogram is plotted immediately beneath the observed seismogram.

with a PE 30–90 instrument in panel (b). The contribution of *pPmP* relative to *PmP* (including the travel time difference from *PmP*) is small and has no apparent effect on the *PmP* seismograms, however the *sPmP* phase contributes strongly as indicated by the arrows. Panel (c) shows a profile of *PmP* + *pPmP* + *sPmP* seismograms displaying the interaction of the various phases with depth, using the same source mechanism. The uppermost seismogram is for an explosion buried at a depth of 0.64 km. While the *sPmP* waveform changes less drastically; its travel time relative to *PmP* is quite significant and is diagnostic of source depth.

Conclusions

There are many important aspects to the problem of seismic event location, especially for smaller magnitude ($M_w < 5$) events which are well recorded – that is, with good signal to noise ratio – only at nearby regional distances, for which developing an accurate regional waveguide model is very critical. With established regionalized earth models, travel-time corrections relative to a reference model can be estimated, based on accurately known event locations, and then consequently be used in the locations of other events. It is important that travel-time tables (or curves) are regionalized in order to determine accurate depths and locations which help reduce

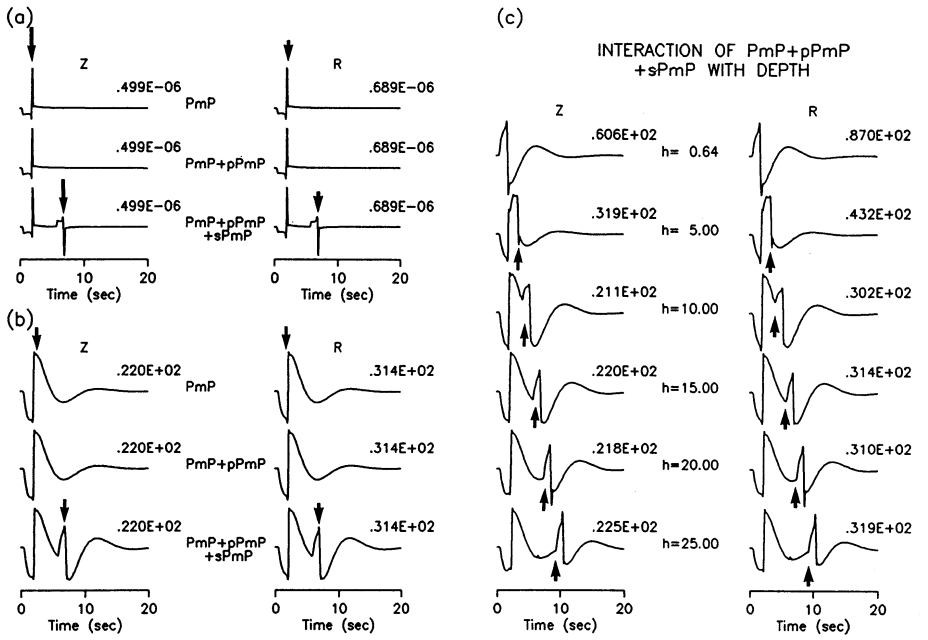

Figure 16

Ray interaction at a regional distance: (a) broadband seismograms: arrows show arrivals of the *PmP* and *sPmP* phases in the seismograms of the first and third row, respectively. Each *PmP* arrival is preceded by a long period P_n, (b) broadband seismograms after being convolved with a Streckeisen instrument, (c) ray interaction at a regional distance, especially of *sPmP* (shown by arrows on each seismogram) as a function of source depth.

the model error which is a source of location error in the teleseismic event location. In general, the most meaningful data for the regionalization are the data from large explosions with known locations and origin times. The next best data are observations from quarry blasts as their locations are also well constrained, but may have less reliable origin times. These data types provide well constrained travel-time information for the shallow focus events. However, in many regions such high quality data are not available. This paper provides a methodology which can be used to establish a set of events, generally with magnitude $M_w \geq 5$, with reliable hypocentral locations and origin times. These events have fairly well determined epicenters teleseismically and often have at least several observations at regional distances. Using the method outlined in this paper, their depths can be constrained to be consistent with both regional and teleseismic seismograms, thereby path calibrations can be used to provide the model-based travel-time estimates for various seismic phases.

In modeling the crustal waveguide of the western Mediterranean region (THIO *et al.*, 1999), we found that the path effects can be quite significant because of the

mixed path contributions from the oceanic and the continental crusts. To locate small events which are expected to be recorded only by a few stations in the region, it is essential that events which are used in the regionalization of the region have accurate source parameters, especially the depths. These events require solutions which are consistent with both regional and teleseismic data. The method adopted by THIO *et al.* (1999), which uses a mixed-path regionalization scheme in conjunction with regional data, can be extended to include the teleseismic data to constrain event depths, and should be useful in regionalization of other similarly complex environments.

The key to the success of obtaining high-quality locations for the master events is in accurately establishing their depths. In general, the locations obtained by minimizing the travel-time residuals of *P* and *S* waves suffer from significant depth error. It is conventionally assumed that error in depth only trades off with the origin time. However, when events' epicenters were relocated with fixed depths, constrained by a combination of teleseismic *P*-wave modeling and regional waveform inversion, using both teleseismic and regional travel times, and a regional crustal model, the locations of seismic events can move significantly with respect to those determined from hypocentral inversions with unconstrained source depths. This was observed in central Asia (WOODS *et al.*, 1999), Pamir Hindu-Kush (SAIKIA *et al.*, 1996a; 1997) and Tibet (ZHAO and HELMBERGER, 1991a). The interaction of the Moho-reflected *PmP* phase with the depth-related, Moho-reflected *sPmP* and *pPmP* phases also provides a useful tool in determining source depth (SAIKIA and HELMBERGER, 1993; LANGSTON, 1996). This is very useful for small events which may be recorded with a strong signal-to-noise ratio only at regional distances. Even if such events are recorded at a few teleseismic stations, the depth phases are not likely to become distinctive, even at short-period. However, it will be possible to estimate the source depth for such small events by analyzing the interaction of the regional phases (SAIKIA and HELMBERGER, 1993; LANGSTON, 1996).

We also discussed a method to locate earthquakes, using an adaptive grid-search algorithm, which was applied to locate earthquakes in the Hindu-Kush region (SAIKIA *et al.*, 1996; ZHU *et al.*, 1997). A similar adaptive grid search technique has also recently been applied to test the hypothesis of locating earthquakes using a sparse network in southern California (ROMANOWICZ *et al.*, 1999). Our proposed method requires that the source depth be estimated by independent means. For smaller ($M_w < 5$) events this involves regional broadband waveform inversion, which in turn requires modeling of the surrounding regional crustal waveguide.

Acknowledgements

The authors are grateful to Donald V. Helmberger of the Caltech Seismological Laboratory for insightful comments at various phases of our investigations. We also

thank the anonymous reviewers and Dr. Howard J. Patton, Los Alamos National Laboratory for their comments which enhanced this paper. This study is supported by the following agencies: Defense Special Weapons Agency (DSWA), Defense Threat Reduction Agency (DTRA) and Department of Energy (DoE); their support is gratefully acknowledged.

REFERENCES

ADAMS, R. D., HUGHES, A. A., and MCGREGOR, D. M. (1982), *Analysis Procedures at the International Seismological Centre*, Phys. Earth Planet. Int. *30*, 85–93.

AKI, K., and RICHARDS, P. G., *Quantitative Seismology – Theory and Methods*, vol. I (W. H. Freeman, New York 1980).

ARVIDSSON, R., and EKSTRÖM, G. (1998), *Global CMT Analysis of Moderate Earthquakes, $M_w \geq 4.5$, Using Intermediate-period Surface Waves*, Bull. Seismol. Soc. Am. *88*, 1003–1013.

BEN-MENAHEM, A., SMITH, S. W., and TENG, T. (1965), *A Procedure for Source Studies from Spectrums of Long-period Body Waves*, Bull. Seismol. Soc. Am. *55*, 203–235.

BILLINGS, S. D., SAMBRIDGE, M. S., and KENNETT, B. L. N. (1994), *Errors in Hypocenter Location: Picking, Model, and Magnitude Dependence*, Bull. Seismol. Soc. Am. *84*, 1978–1990.

BONDAR, ISTVAN (1998), *PIDC Ground Truth Event Bulletin Technical References*, Technical Report CMR-98/21, Center for Monitoring Research, Alexandria, VA.

DI LUCCIO, F., JONES, L., ZHU, L., and HAUKSSON, E. (1998), *Comparison of Waveform Inversions and Arrival Time Techniques to Resolve Earthquake Depths and Focal Mechanisms in Southern California*, EOS, vol. *79*, no. 45, 603 pp.

DREGER, D. S., and HELMBERGER, D. V. (1993), *Determination of Source Parameters at Regional Distances with Single Station or Sparse Network Data*, J. Geophys. Res. *98*, 8107–8126.

DZIEWONSKI, A. M., CHOU, T.-A., and WOODHOUSE, J. H. (1981), *Determination of Earthquake Source Parameters from Waveform Data for Studies of Global and Regional Seismicity*, J. Geophys. Res. *86*, 2825–2852.

DZIEWONSKI, A. M., and STEIM, J. (1982), *Dispersion and Attenuation of Mantle Waves through Waveform Inversion*, Geophys. J. R. Astron. Soc. *70*, 503–527.

ENGDAHL, E. R., VAN DER HILST, R., and BULAND, R. (1998), *Global Teleseismic Earthquake Relocation with Improved Travel Times and Procedures for Depth Determination*, Bull. Seismol. Soc. Am. *88*, 722–743.

ENGDAHL, E. R., *Development of an archive of seismic ground truth events globally in support of monitoring under the CTBT*. In *Proc. 20th Ann. Seis. Res. Symp.* (eds. Fantroy, J., Heatley, D., Warren, J., Chavez, F., and Meade, C.) (DoD/NTP, Alexandria, VA, and DoE, Washington, DC 1998) pp. 11–18.

GAUR, V. K., and PRIESTLEY, K. F. (1997), *Shear-wave Velocity Structure beneath the Archean Granites around Hyderabad, Inferred from Receiver Function Analysis*, Academy Proceed. Earth. Planet. Sci. *106*, 1–8. IIS, Bangalore, India.

GEE, L. S., NEUHAUSER, D. S., DREGER, D. S., and PASYANOS, M. E. (1996), *Real-time Seismology at UC Berkeley: The Rapid Earthquake Data Integration Project*, Bull. Seismol. Soc. Am. *86*, 936–945.

GHOSE, S. M., HAMBURGER, W., and AMMON, C. J. (1998), *Source Parameters of Moderate-sized Earthquakes in the Tien Shan, Central Asia from Regional Moment Tensor Inversion*, Geophys. Res. Lett. *25*, 3181–3184.

GUPTA, I. N., ZHANG, T. R., and WAGNER, R. A. (1998), *Low-frequency Lg from NTS and Kazakh Nuclear Explosions – Observations and Interpretation*, Bull. Seismol. Soc. Am. *87*, 1115–1125.

HASKELL, N. A. (1962), *Crustal Reflection of Plane P and SV Waves*, J. Geophys. Res. *67*, 4751–4767.

HELMBERGER, D. V., and ENGEN, G. R. (1980), *Modeling the Long-period Body Waves from Shallow Earthquakes at Regional Ranges*, Bull. Seismol. Soc. Am. *70*, 1699–1714.

HELMBERGER, D. V. (1973), *Numerical Modeling of Long-period Body Waves from Seventeen to Forty Degrees*, Bull. Seismol. Soc. Am. *63*, 633–646.

HELMBERGER, D. V. (1972), *Long-period Body-wave Propagation from 4° to 13°*, Bull. Seismol. Soc. Am. *62*, 325–341.

HOLT, W. E., and WALLACE, T. C. (1989), *Crustal Thickness and Upper Mantle Velocities in the Tibetan Plateau Region from the Inversion of Regional P_{nl} Waveforms: Evidence for a Thick Upper Mantle Lid Beneath Southern Tibet*, J. Geophys. Res. *95*, 12,499–12,525.

HUDSON, J. A. (1969), *A Quantitative Evaluation of Seismic Signals at Teleseismic Distances. I: Radiation from Seismic Sources*, Geophys. J. R. Astron. Soc. *18*, 233–249.

LANGSTON, C. B. (1996), *The SsPmp Phase in Regional Wave Propagation*, Bull. Seismol. Soc. Am. *86*, 133–143.

LANGSTON, C. A., and HELMBERGER, D. V. (1975), *A Procedure for Modeling Shallow Dislocation Sources*, Geophys. J. R. Astron. Soc. *42*, 117–130.

LEFEVRE, L. V., and HELMBERGER, D. V. (1989), *Upper Mantle P-velocity Structure of the Canadian Shield*, J. Geophys. Res. *94*, 17,749–17,765.

LEVSHIN, A. L. (1985), *Effects of Lateral Inhomogeneities on Surface Wave Amplitude Measurements*, Annales Geophysicae *3*, 511–518.

MOONEY, W. D., and LI, S., *Crustal structure of China from deep seismic sounding profiles*. In *Proc. 19th Ann. Seis. Res. Symp. on Monitoring a CTBT* (eds. Shore, M., Jih, R. S., Dainty, A., and Erwin, J.) (DSWA, Alexandria, VA; AFTAC, Patrick AFB, FL; and DoE, Washington, DC 1997) pp. 104–114.

MOONEY, W. D., LASKE, G., and MASTER, T. G. (1998), *Crust 5.1: A Global Crustal Model at 5° × 5°*, J. Geophys. Res. *103*, 727–747.

NAKANISHI, I., and KANAMORI, H. (1982), *Effects of Lateral Heterogeneity and Source Process Time on the Linear Moment Tensor Inversion of Long-period Rayleigh Waves*, Bull. Seismol Soc. Am. *72*, 2063–2080.

NELSON, M. R., MCCAFFREY, R., and MOLNAR, P. (1987), *Source Parameters for 11 Earthquakes in the Tien Shan, Central Asia, Determined by P and SH Waveform Inversion*, J. Geophys. Res. *92*, 12,629–12,648.

PATTON, H. J. (1998), *Bias in the CMT Moment for Central Asian Earthquakes: Evidence from Regional Data*, J. Geophys. Res. *89*, 6929–6940.

PATTON, H. J., and WALTER, W. R. (1993), *Regional Moment: Magnitude Relations for Earthquakes and Explosions*, Geophys. Res. Lett. *20*, 277–280.

PRIESTLEY, K. F., and PATTON, H. J. (1997), *Calibration of $m_b(P_n)$, $m_b(L_g)$ Scales and Transportability of the M_0:m_b Discriminant to New Tectonic Regimes*, Bull. Seismol. Soc. Am. *87*, 1083–1099.

RITMESA, J., and LAY, T. (1993), *Rapid Source Mechanism Determination of Large $M_w > 5$ Earthquakes in the Western United States*, J. Geophys. Res. *20*, 1611–1614.

RODGER, A. J., and SCHWARTZ, S. Y. (1998), *Lithospheric Structure of the Qiangjang Terrane, Northern Tibetan Plateau, from Complete Regional Waveform Modeling, Evidence for Partial Melt*, J. Geophys. Res. *103*, 7137–7152.

RÖHM, A. H. E., TRAMPERT, J., PAULSSEN, H., and SNIEDER, R. K. (1999), *Bias in Reported Seismic Arrival Times Deduced from the ISC Bulletin*, Geophys. J. Int. *137*, 163–174.

ROMANOWICZ, B., DREGER, D., UHRHAMMER, R., and PASYANOS, M., *Earthquake locations using sparse regional broadband data*. In *Workshop on IMS Location Calibration, Tech. Doc.* (ed. Ringdal, F.) (NORSAR, Oslo 1999).

ROMNEY, C., BROOKS, B. G., MANSFIEKL, R. H., CARDER, D. S., JORDAN, J. N., and GORDON, D. W. (1962), *Travel Times and Amplitude of Principal Body Phases Recorded from Gnome*, Bull. Seismol. Soc. Am. *52*, 1057–1074.

RUSSIAN FEDERATION/UNITED STATES CALIBRATION WORKING GROUP (1998), *Evaluation of the IMS location accuracy of large chemical and nuclear explosions in Northern Eurasia and North America using regional and global P_n Travel-time Tables*. In *Proc. 20th Ann. Seis. Res. Symp.* (eds. Fantroy, J., Heatley, D., Warren, J., Chavez, F., and Meade, C.) (DoD/NTP, Alexandria, VA, and DoE, Washington, DC 1998) pp. 104–113.

RYABOY, V. (1999), *Application of 3-D crustal and upper-mantle velocity models in North America for location of regional seismograms*. In *Workshop on IMS Location Calibration, Tech. Doc.* (ed. Ringdal, F.) (NORSAR, Oslo 1999).

SAIKIA, C. K., ZHU, L., WOODS, B. B., and THIO, H. K., *Path calibration and source characterization in and around India*. In *Proc. 21st Ann. Seis. Res. Symp.: Technologies for Monitoring the CTBT*, vol. I, LA-UR-99-4700 (DoD, Alexandria, VA; and DoE, Washington, DC 1999) pp. 243–253.

SAIKIA, C. K., WOODS, B. B., THIO, H. K., SONG, X., and HELMBERGER, D. V. (1997), *Path Calibration, Source Estimation and Regional Discrimination for the Middle East and the Mediterranean*, Scientific Rept. 3, DSWA-TR-98-70 (DSWA, Special Programs Office, Alexandria, VA) 110 p.

SAIKIA, C. K., WOODS, B. B., THIO, H. K., ZHU, L., and HELMBERGER, D. V. (1996a), *Path Calibration, Source Estimation and Regional Discrimination for the Middle East: An Application to the Hindu-Kush Region*, Scientific Rept. No 1, PL-TR-96-2069 (Phillips Laboratory, HAFB, MA) 130 pp.

SAIKIA, C. K., THIO, H. K., WOODS, B. B., SONG, X., ZHU, L., and HELMBERGER, D. V. (1996b), *Path Calibration, Source Estimation and Regional Discrimination for the Middle East: An Application to the Hindu-Kush and Western Mediterranean Regions,* Scientific Rept. No. 2, PL-TR-96-2307 (Phillips Laboratory, HAFB, MA) 205 pp.

SAIKIA, C. K. (1994), *Modified Frequency-wavenumber Algorithm for Regional Seismograms using Filon's Quadrature – Modeling of L_g Waves in Eastern North America*, Geophys. J. Int. *118*, 142–158.

SAIKIA, C. K., and HELMBERGER, D. V. (1993), *Broadband Modeling of Regional Seismograms in Asia and Development of Low-magnitude Event Discrimination*, Final Rept. WCCP-R-93-04 (Phillips Laboratory, Kirtland AFB, NM) 135 pp.

SAIKIA, C. K., and BURDICK, L. J. (1991), *Fine Structure of P_{nl} Waves from Explosions*, J. Geophys. Res. *96*, 14,383–14,401.

SAIKIA, C. K., and HERRMANN, R. B. (1985), *Application of Waveform Modeling to Determine Focal Mechanisms of Four 1982 Miramichi Aftershocks*, Bull. Seismol. Soc. Am. *75*, 1021–1041.

SINGH, S. K., SANTOYO, M. A., and PACHECO, J. (1995). *Intermediate-depth Earthquakes in Central Mexico: Implications for Plate Waves*, Geophys. Res. Lett. *22*, 527–530.

SIPKIN, S. A. (1982), *Estimation of Earthquake Source Parameters by the Inversion of Waveform Data: Synthetic Seismograms*, Phys. Earth Planet. Int. *30*, 242–259.

SONG, X. J., HELMBERGER, D. V., and ZHAO, L. (1996), *Broad-band Modeling of Regional Seismograms: The Basin and Range Crustal Structure*, Geophys. J. Int. *125*, 15–29.

STEIN, S., and WIENS, D. A. (1986), *Depth Determination for Shallow Teleseismic Earthquakes: Methods and Results*, Rev. Geophys. *24*, 806–832.

TAYLOR, S. R. (1995), *Analysis of High-frequency P_g/L_g Ratios from NTS Explosions and Western U.S. Earthquakes*, Bull. Seismol. Soc. Am. *86*, 1042–1053.

TENG, T., and BEN-MENAHEM, A. (1962), *Mechanisms of Deep Earthquakes from Spectrums of Isolated Body-wave Signals. 1. The Banda Sea Earthquake of March 21, 1964*, J. Geophys. Res. *70*, 5157–5170.

THIO, H. K., SONG, X., SAIKIA, C. K., HELMBERGER, D. V., and WOODS, B. B. (1999), *Seismic Sources and Structure Estimation in the Western Mediterranean Using a Sparse Broadband Network*, J. Geophys. Res. *104*, 845–861.

THIO, H. K., and KANAMORI, H. (1995), *Moment Tensor Inversions for Local Earthquakes Using Surface Waves Recorded at TERRAscope*, Bull. Seismol. Soc. Am. *85*, 1021–1038.

VÖGFORD, K. S. (1997), *Effects of Explosion Depth and Earth Structure on the Excitation of L_g Waves: S* Revisited*, Bull. Seismol. Soc. Am. *87*, 1100–1114.

WALLACE, T. C., HELMBERGER, D. V., and MELLMAN, G. R. (1981), *A Technique for the Inversion of Regional Data in Source Parameter Studies*, J. Geophys. Res. *86*, 1679–1685.

WALTER, W. R., MAYEDA, K. M., and PATTON, H. J. (1995), *Phase and Spectral Ratio Discrimination between NTS Earthquakes and Explosions. Part I: Empirical Observations*, Bull. Seismol. Soc. Am. *85*, 1050–1067.

WOODS, B. B., SAIKIA, C. K., and THIO, H. K. (1999), *Extending regional waveform modeling to shorter periods to improve the location and identification of small seismic sources*. In *Proc. 21st Ann. Seis. Res. Symp.: Technologies for Monitoring the CTBT*, vol. I, LA-UR-99-4700 (DoD, Alexandria, VA; and DoE, Washington, DC 1999) pp. 303–311.

WOODS, B. B., SAIKIA, C. K., THIO, H. K., and PATTON, H. J. (1998), *Focal Depths and Source Parameters for Earthquakes in Northwest China*, Tech. Rept. (LANL, Los Alamos).

WOODS, B. B., and HARKRIDER, D. G. (1995), *Determining Surface Wave Magnitudes from Regional NTS Data*, Geophys. J. Int. *120*, 474–498.

WOODS, B. B., HELMBERGER, D. V., and KEDAR, S. (1993), *M_L:M_0 as a Regional Seismic Discriminant*, Bull. Seismol. Soc. Am. *83*, 1167–1183.

ZANDT, G., BECK, S. L., RUPPERT, S. R., AMMONS, C. J., ROCK, D., MINAYA, E., WALLACE, T. C., and SILVER, P. G. (1996), *Anomalous Crust of the Bolivian Altiplano, Central Andes: Constrains from Broadband Regional Seismic Waveforms*, Geophys. Res. Lett. *23*, 1159–1162.

ZHAO, L.-S., and HELMBERGER, D. V. (1994), *Source Estimation from Regional Broadband Seismograms*, Bull. Seismol. Soc. Am. *84*, 91–94.

ZHAO, L.-S., and HELMBERGER, D. V. (1992), *Source Retrieval from Broadband Regional Seismograms: Hindu Kush Region*, Phys. Earth Planet. Int. *78*, 69–95.

ZHAO, L.-S., and HELMBERGER, D. V. (1991a), *Geophysical Implications from Relocations of Tibetan Earthquakes: Hot Lithosphere*, Geophys. Res. Lett. *18*, 2205–2208.

ZHAO, L.-S., and HELMBERGER, D. V. (1991b), *Broadband Modeling along a Shield Path. Harvard Recordings of the Saguenay Earthquake*, Geophys. J. Int. *105*, 301–312.

ZHU, L., HELMBERGER, D. V., SAIKIA, C. K., and WOODS, B. B. (1997), *Regional Waveform Calibration in the Pamir-Hindu Kush Region*, J. Geophys. Res. *102*, 22,799–33,813.

ZHU, L., and HELMBERGER, D. V. (1996), *Advancement of Source Retrieval from Broadband Regional Seismograms*, Bull. Seismol. Soc. Am. *86*, 1634–1641.

(Received September 13, 1999, revised May 12, 2000, accepted May 31, 2000)